

We are IntechOpen, the world's leading publisher of Open Access books Built by scientists, for scientists

6,900

Open access books available

186,000

International authors and editors

200M

Downloads

Our authors are among the

154

Countries delivered to

TOP 1%

most cited scientists

12.2%

Contributors from top 500 universities



WEB OF SCIENCE™

Selection of our books indexed in the Book Citation Index
in Web of Science™ Core Collection (BKCI)

Interested in publishing with us?
Contact book.department@intechopen.com

Numbers displayed above are based on latest data collected.
For more information visit www.intechopen.com



Molecular Dynamics Simulation Study on the Mechanical Properties and Fracture Behavior of Single-Wall Carbon Nanotubes

Keka Talukdar and Apurba Krishna Mitra

*Department of Physics, National Institute of Technology, Durgapur
India*

1. Introduction

Tremendous research motivation has been observed in the composite science and technology since the discovery of carbon nanotubes by Sumio Iijima (Iijima, 1991). Carbon nanotubes are highly crystallized tubular allotropes of carbon with hexagonal pattern repeating itself in space. The in-plane C-C bond is strong covalent σ bond. In contrary, there exists a weak π bond out of plane which acts in between the shells of a multi-wall carbon nanotube or in between different single-wall carbon nanotubes in a bundle. The combination of the high strength and high elastic modulus along the axial direction and the low density with high aspect ratio of the tubes has imparted in them excellent mechanical properties such that they may be used as reinforcing fibers in a polymer matrix to prepare low weight, high strength structural composites. As a component of a fiber-filled composite, the exact knowledge of the mechanical characteristics of the carbon nanotubes is necessary to tailor them for specific use. However, the proper strength and failure behavior of the nano materials can only perfectly be understood by atomistic simulation. In the nano regime, the continuum mechanics is inadequate and an atomistic description of the system is necessary. Moreover the carbon nanotubes are found to consist of various types of defects. Defects present inside their structure often result in some very complex phenomena in their failure process in the atomic scale which can be handled only by atomistic simulation. Here the power of molecular dynamics simulation technique is exploited in investigating the mechanical characteristics of various types of defect-free as well as defective tubes with a varying number of Stone-Wales defects with different combinations. The effect of interlayer interaction between different single-wall tubes in a bundle and the role of potential functions in the mechanical behavior of different carbon nanotubes are also investigated here.

2. Theoretical predictions and experimental observations

Nanoelectromechanical systems or super strong composite materials, which are of great interest in the present days, can be realized in practice by fabrication of materials using carbon nanotubes (CNTs). The choice of CNTs in these fields is found to be very much beneficial for their tremendous high strength and low density. Young's modulus of a solid depends on the nature of the chemical bonding of the constituent atoms. Due to the

presence of strong covalent σ bond the axial Young's modulus should be equal to the in plane elastic modulus of graphite (1.04 TPa). Measurements with HRTEM or AFM reveal that CNTs have high Young's modulus which is close to 1 TPa, i.e. 100 times that of steel. All experimental observations (Krishnan et al., 1998; Salvétat et al., 1999a, 1999b; Treacy et al., 1996;) predict such high stiffness of the CNTs or their bundles. Very high Young's modulus of 2.8–3.6 TPa, for SWCNT and 1.7–2.4 TPa for MWCNT have also been observed in some studies (Lourie et al., 1998). Y value of 1.28 ± 0.59 TPa was found in one investigation (Wong et al., 1997). Scanning electron microscopy was used by Yu et al. (Yu et al., 1999a, 2000b, 2000c) for direct measurement of the tensile properties. Young's modulus obtained ranges from 0.32–1.47 TPa with a mean of 1.002 TPa for single-wall carbon nanotubes (SWCNTs) and 0.27–0.95 TPa for multi-wall carbon nanotubes (MWCNTs).

But the prediction of their mechanical properties (Batra & Sears, 2007; Belytschko et al., 2002; Chou, et al., 2010; Coluci et al., 2007; Dereli & Özdoğan, 2003; Liew et al., 2004; Yakobson et al., 1996) often ends with some uncertainties especially due to some unavoidable defects produced in them during their production, purification or functionalization. Stone-Wales (SW) defects (Stone & Wales, 1986), vacancies, pentagons, heptagons, lattice-trapped states, ad-dimers etc. are many types of defects that can appear in the CNT structure. Influence of defects can be observed in the mechanical properties of CNTs as well as in their electronic or magnetic properties. However, the effect of Stone-Wales defects has been investigated by many researchers (Belytschko et al., 2002; Chandra et al., 2004; Nardelli et al., 1998; Pozrikidis, 2009; Song et al., 2006; Troya et al., 2003; Tunvir et al., 2008) to obtain widely varying results. Such type of defect is produced by 90° rotation of a C-C bond and thus producing two pentagons and two heptagons by conversion from four hexagons of carbon atoms. No matter what the process or potential adopted, reduction of failure strength and ductility has been reported by most of the authors. Some authors observed that chemical reactivities were enhanced for a defective zigzag SWCNT compared to and planar graphene (Picozzi et al., 2004). The role of vacancy defects or holes on the mechanical properties of CNTs was studied in many theoretical investigations such as that of Mielke et al. (Mielke et al., 2004), Xiao & Hou (Hou & Xiao, 2007) and Wang et al. (Wang et al., 2007). Decreasing effects on the failure stress and failure strain along with the scattering of stress values were reported by Troya et al. (Troya et al., 2003) for the introduction of 1, 2 and 5 adjacent and diagonal defects. Semiempirical quantum mechanical calculations of Troya included MSINDO and PM3 methods. They used 2nd generation Brenner potential for simulation. Mielke et al. (Mielke et al., 2004) performed MD simulation in three different approaches- DFT on the plane wave basis, PM3 approach and MTBG2. They took pristine as well as defective CNTs with one and two atom vacancies.

The role of defects on carbon nanotube elastic moduli and failure behavior was studied by tight binding molecular dynamics simulation by Haskins et al. (Haskins et al., 2007). Molecular simulation was used by Yang et al. (Yang et al., 2007) to determine the fracture strength of single-wall carbon nanotubes containing different concentrations of randomly distributed point defects. Another attempt to explain the discrepancies between the theoretical and the experimental results in predicting the mechanical properties of CNTs was made by Huq et al. (Huq et al., 2008). Shtogun and Woods (Shtogun & Woods, 2010) has calculated the mechanical properties of radially deformed defective single-wall carbon nanotube by first principle density functional theory calculations. Two different modes of formation of SW defects (mode 1 and mode 2, also referred as SW-A and SW-B) were

considered by molecular mechanics model. Pozrikidis (Pozrikidis, 2009) has shown that inclined, axial and circumferential defect orientations have a strong influence on the mechanical response of zigzag and armchair SWCNTs. An attempt to explain the reason of scattering in data of the mechanical properties of CNTs was made by Tunvir et al (Tunvir et al., 2008) with Morse potential. To investigate the interference effect of spatial arrangements between two neighboring vacancy and SW defects with respect to the loading direction, their relative distances as well as their local orientations were varied and the results were compared. But they considered the defects in the middle of a (10, 10) SWCNT and the defects were considered in only one side of the tube.

In 1995 Ebbesen & Takada (Ebbesen & Takada, 1995) got an experimental evidence of topological defects such as Stone-Wales defects in CNTs. Miyamoto et al. (Miyamoto et al., 2004) made an experimental identification of SW defects in CNT samples. Thus the experiments established the facts that the lower values of Young's modulus and tensile strength of CNTs originated because of the presence of defects in them, in particular the SW defects.

The enhancement in the mechanical performance of materials is reported in the literature (Dalton et al., 2003; Koizol et al, 2007; Mora et al., 2009;) while preparing composites using CNTs as reinforcing agents. Based on finite element method, MD simulation study (Kuronuma et al., 2010) has been done to explore the fracture behavior of cracked carbon nanotube based polymer composites. Seo et al. (Seo et al., 2010) concluded that the MWCNTs were the good and appropriate materials to improve elastic behavior of the composites with a large increase in their flexural strength and Young's modulus in the tune of about 60%. In spite of so much research attempts discussed above, there still exists enough scope of investigation about the mechanical properties of the CNTs and an elaborate study can only lead to better design of high-strength CNT-composites.

3. The aim of this study

All types of carbon nanotubes can be used for low weight structural composites. NASA is developing materials using CNTs for space applications, where weight driven cost is the major concern (Despres et al., 1995, Iijima et al., 1996). Sufficient improvement in the research work in this field has been achieved to enhance the adhesion of the CNTs with the host to build composite materials for various purposes (Andrews et al., 1999; Chae et al., 2006; Kearns and Shambaugh, 2002). During processing or purification, different chemical groups are attached with the CNTs either via "end and defect-site" or by "sidewall functionalization" process. The chemical attachment of the less curved sidewalls usually requires the presence of sidewall defects such as Stone-Wales defects (Balasubramanian & Burghard, 2005; Banerjee et al., 2005). For better bonding of carbon nanotubes with polymer matrix in a CNT-polymer composite, suitable functionalization of the CNTs is essential. Different types of chemical functional groups can be attached (Kang et al., 2010; Qi et al., 2003) in these processes without hampering nanotube properties. So the presence of defects in the CNT structure is not always degrading.

Using monochromatic light or electron beam, suitable number of defects can be produced in the CNT structure for specific applications. A review (Krasheninnikov & Banhart, 2007) on the engineering of CNTs and other carbon materials with electron ion beams discuss the recent advancements in this respect. Defects can serve the purpose of grafting functional groups directly at the defect site (Canto et al., 2011). Addition reaction is most favorable in

the position of Stone-Wales defects at the carbon-carbon double bond. Again attaching functional groups to the CNTs is necessary to achieve proper adhesion of them with the polymer matrix while forming composites. Electron beam exposure at high temperatures induces structural defects in CNTs which promote the joining of tubes via cross-linking of dangling bonds and thus producing Y or T junctions. This fact is both experimentally and theoretically proved by Terrones et al. (Terrones et al., 2002). Defect-induced junctions between single-wall, double-wall carbon nanotubes and also between metal crystals are possible (Manzo et al., 2010) as electron irradiation produces structural transformation in the CNTs and metal atoms (Banhart, 1999). Fusion of two (5, 5) SWCNTs into a (10, 10) tube via a zipper mechanism by SW transformation is also reported by Yoon et al. under HRTEM (Yoon et al., 2004). Under electron irradiation, the experimental and theoretical evidence of the change of CNT's diameter is also another consequence of the artificial production of defects (Ajayan et al., 1998). So production of defects in certain amount and in specific positions of a CNT is not a difficult task with the newly developed experimental techniques.

Defects were previously thought to be only unwanted, but now it is shown that they can be controllably produced for preparing novel nanodevices. So the need to identify and quantify them is also required. Measurements done by polarization dependent scanning transmission X-ray microscopy (Felten et al., 2010) or Raman spectroscopy (Miyata et al., 2011) can now identify and quantify defects. Defect spacing can further be varied by varying the synthesis technique (Fan et al., 2005).

Observing the new trends in the progress in the defect-controlled manipulation of the nanotube properties in various fields of science and technology, we have critically investigated their mechanical properties involving two major defects, mainly SW defects. As the SWCNTs have cylindrical geometry, defects may arise on its surface anywhere. Thus defects may appear not only in one side but they may be situated opposite to each other. Keeping this in mind, more than one defect are considered at different positions of a zigzag (10, 0), chiral (5, 3) and armchair (5, 5) SWNTs with varying separating distances and with different separating angles to simulate them in atomic scale. Also 2nd generation Tersoff-Brenner (Brenner et al., 2002) potential is incorporated in our study which can explain nicely the creation and destruction of bonds in a CNT structure. Defects are distributed in all parts of the tube and moreover, diagonal, overlapping and neighboring defects are taken along with many other possible arrangements. Fracture modes are modeled and compared with a detailed study of the mechanical response of the tubes viz, young's modulus, failure strength and ductility.

Experimental data (Yu et al., 2000c) for a single-wall carbon nanotube bundle under tensile load show that the Young's modulus can be as high as 1.47 TPa and tensile strength may range from 13-53 GPa. In spite of so many attempts to explain the discrepancies between the theoretical and experimental data regarding the mechanical properties of SWCNTs, some observed discrepancies between theory and experiment are still unanswered. SWCNTs have a natural tendency to form bundles and thus in the most of the experiments undertaken by various investigators, SWCNT bundles have been used as samples. So we must take into account the influence of bundle formation in our calculations of mechanical properties of SWCNTs. In this work, we have compared the observed mechanical properties of three different types of SWCNTs separately and also the bundles of each type and a bundle of their mixture. The results are explained with the overlapping of density of states (DOS) of

the CNTs in a bundle. So this is an attempt to carry out more realistic theoretical investigations to facilitate comparison with experimental data. 2nd generation reactive empirical bond order potential (Brenner et al., 2002) is adopted for simulation. For this study we have restricted the potential to be smoothed-off at the cut-off region. Lennard-Jones 6-12 potential (Lennard-Jones, 1924) function is adopted for interlayer interaction.

To explain the above discrepancies, different types of SWCNTs are simulated using three different potential functions and the results are compared.

4. Atomistic modeling and simulation

By atomistic modeling one can understand the interaction between the constituent molecules of a material and thus the behavior of the material with various external constraints, their deformation and failure process can also be understood. Starting from the simple laws of Physics to describe the position and momentum of each atom in a material and solving the equations of motion of the system of atoms or molecules, one can obtain the dynamic behavior of all the particles of the system. Thermodynamical behavior of gases and liquids (Alder & Wainwright, 1957; Alder & Wainwright, 1959; Allen & Tildesly, 1989; Rahman, 1964) was the first, where molecular dynamics simulation was performed. Later, this process has been used to find the mechanical behavior of solids. The failure process of solids is associated with so many computational complexities that modeling and simulation have now become a very exciting area of research. At first, a mathematical model is to be developed for a physical problem. Then the equations resulting from that model building (Ashby, 1996) are to be solved. The model should be such that it should be able to capture the physical features of the problem. Sidney Yip of MIT (Yip, 2005) has stated that modeling is the physicalization of a concept, simulation its computational realization. Modeling requires the knowledge about the physics of the system i.e. about its constituents or the behavior of the particles. Simulation requires the technique to solve enormous numerical equations related to the complicated systems. The behavior of cracks, dislocations, grain boundary processes can be very successfully investigated by atomistic modeling (Buehler, 2008). In modern materials modeling this process has gained immense importance. Any complex problem can be solved by knowing Newton's laws and the nature of interaction of the atoms. In the present work mechanical properties of the CNTs are investigated by modeling and simulation. Nowadays, researchers have considered the computer as a tool to do experiment, similar as experimentalists do in their laboratory. Computational experiments thus need to build a suitable model of a physical problem, set up some equations to represent the problem, run simulation and to interpret the results of the simulation process.

4.1 Molecular dynamics simulation

Molecular dynamics simulation is a form of computer simulation in which atoms and molecules are allowed to interact for a period of time by approximations of known physics, giving a view of the motion of the particles. Position and momentum of each particle is updated using a suitable algorithm. In materials science, this is a very effective process. We call molecular dynamics simulation a computer simulation technique where the time evolution of a set of interacting atoms is followed by integrating their equations of motion. Material behavior and their deformation are described in atomistic modeling. The purpose of molecular dynamics simulation is to understand the properties of assemblies of molecules

in terms of their structure and the microscopic interactions between them. Something new, which cannot be found in other ways, can be learnt by simulation.

4.2 Present method of simulation

We have performed MD simulation using the software 'Brenner code' which is an open source code and which has been customized and modified as necessitated by our scheme of work. The coordinates of a carbon nanotube generated in the program can be used for simulation. The programs are all written in FORTRAN language. All programs are to be compiled separately to run the main program. Microsoft developer studio is used as the platform of manipulating programs. Time step of 0.5 fs is chosen for the molecular dynamics simulation presented here. We have tested that slight changes in the time step affect the simulation result negligibly. Also The evolution of the system energy with respect to time is noticed and it is observed that 30000-50000 time steps are required to achieve convergence in energy minimization and hence to get equilibrium condition. However, simulation can be run using other software also, like TINKER, LAMMPS etc.

A thermostat is required to lead a system to a desired temperature i.e. to enable a NVT or NPT ensemble. To modify the equations of motion to obtain a specific thermodynamical ensemble, the velocities of the atoms are rescaled by a scaling factor. We have used Berendsen thermostat (Berendsen et al., 1984) in this study to maintain a fixed temperature. In this thermostat, velocity is rescaled by a factor $\lambda = \sqrt{T_0/T(t)}$

In each step velocity is rescaled so that the rate of increase of temperature is proportional to the difference in temperature; $dT(t)/dt = 1/\tau (T_0 - T(t))$

So the scale factor is given by, $\lambda = [1 + \Delta t/\tau (T/T_0 - 1)]^{1/2}$

when Δt is the time step and τ is a coupling constant. It is called rise time which gives the strength of the coupling of the system with the hypothetical heat bath at temperature T_0 .

5. Verification of the dependence of mechanical response of single walled carbon nanotubes with the position and arrangement of stone-wales defects

5.1 Theoretical method

The two pentagons and two heptagons that are produced by the 90° rotation of a C-C bond in the honeycomb structure of a SWCNT may be oriented in different manner. The tube symmetry and the inclination of the axis joining the pentagons or heptagons with the tube axis decide whether the excess strain of formation of defect is released or not while straining the tube. Three different SWCNTs are taken and analyzed in our study. The zigzag, chiral and armchair tubes are 42.5, 59.6 and 49.19 Å long respectively with aspect ratios 10.9, 21.75 and 14.5. The zigzag and armchair tubes contain 400 atoms and the chiral tube contains 392 atoms as a whole. Berendsen thermostat is used to allow small changes in the velocities of the atoms such that temperature of the system reaches a value close to 300K. The tubes are stretched in the axial direction keeping other end fixed. By stretching the tubes in small strain increments, the equilibrium potential energy were calculated by simulation at first in absence of any defect and then with 1, 2, 3 and 4 defects at different positions of the tubes. Stretch is applied along the axis of the tubes. No other constraint is there in other directions and force is zero in any other direction.

Stress is calculated from the energy-strain curve as $\sigma = 1/V (dE/d\varepsilon)$ where σ is the longitudinal stress, V the volume of the tube, ε the strain and E the strain energy of the tube. Volume of the tube is found as $V = 2\pi r \delta r l$ where r is the inner radius of the tube, δr its wall

thickness and l the length of the tube. We have taken δr as 0.34 nm, which has been the standard value, used by most of the authors. To calculate stress from the energy-strain curve we have used a linear relationship for the elastic region and appropriate non-linear equations for the segments of high strain deformation regions. Young's modulus is found from the slope of the linear portion of the stress-strain curve. By changing the (z, r, θ) values, defects are created at different positions of the same tube. θ is changed by 90° from its first value to form two oppositely directed defects. To produce two diagonal defects θ is changed by 45° and z is adjusted to the desired value.

5.2 Characteristics of defect free tubes

With Brenner's 2nd generation REBO potential an armchair SWCNT shows remarkable ductility of 32% and tensile strength of 196.3 GPa [Fig 1]. A chiral tube breaks at 30% strain while its failure stress is calculated to be 149.88 GPa. The ductility and failure stress of a zigzag tube, in contrary, are much less and that are 18% and 115.4 GPa respectively. Linear elastic region extends upto 7% strain, beyond which the nature of the curve changes to non-linearity. Young's modulus is found for the pristine tube as 1.06 TPa for a zigzag tube, 0.891 for a chiral tube and 0.814 for an armchair tube. Our calculation matches with the experimental values of failure stress by Demczyk (Demczyk et al., 2002) which is 150 ± 45 GPa. Young's modulus value is also close to the experimental value of 1.28 TPa by Wong et al. (Wong, 1997) and 1.25 TPa by Krishan et al. (Krishnan et al., 1998). Maximum strain can be compared with the results of quantum mechanical calculations (Ozaki et al., 2000; Troya et al., 2003) though 10-13% maximum strain and failure stress between 13-52 GPa were observed by Yu et al. (Yu et al., 2000c) experimentally. Fracture of a zigzag SWNT [Fig 2(a)] is found to be brittle in our calculation. As shown in Fig 2(b) and 2(c), failure patterns are not so sharp for a chiral and an armchair tube.

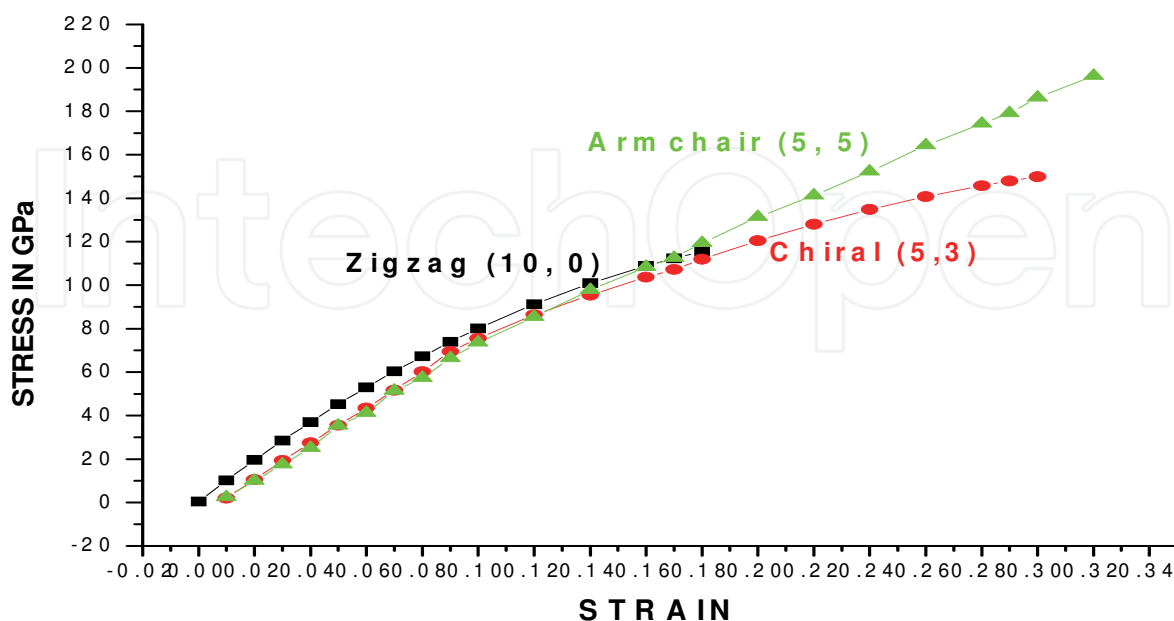


Fig. 1. Stress-Strain curves for defect free SWCNTs

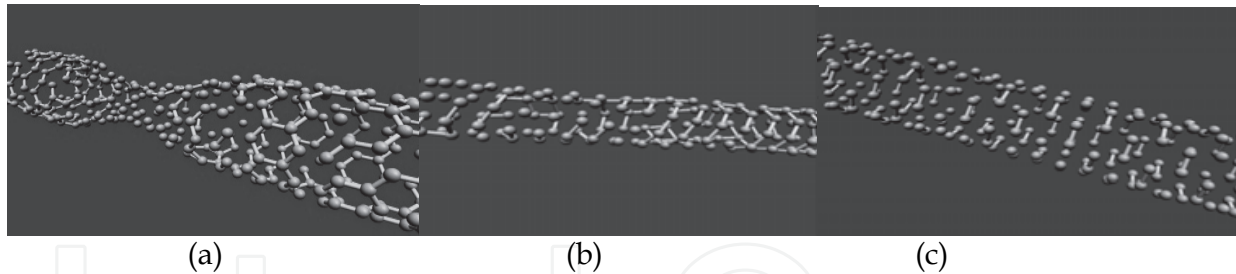


Fig. 2. Fracture patterns of a defect free (a) zigzag (10, 0) (b) Chiral (5, 3) and (c) Armchair (5, 5) SWCNTs

5.3 Modeling of defects

A 5/7/7/5 defect is realised theoretically by rotation of a C-C bond by 90° and thus converting two pair of hexagons to two pentagons and two heptagons. Single defect is created in any desired place by adjusting (z, r, θ) values. For more than one defect z values are changed to produce separated defects and orientation between two defects or oppositely situated defects are produced by changing θ . Symmetric defects mean that they are situated symmetrically on both sides of $z=0$ position. Same θ for a number of defects produces some defects on the same line. Where θ varies by 180° , oppositely situated defects are produced. Thus, for four different combinations of z, r and θ as $(-4.26, 3.91, 90)$, $(-12.78, 3.91, 90)$, $(4.26, 3.91, -90)$, $(12.78, 3.91, -90)$, four symmetrical but oppositely situated defects are produced. Fig 3 shows a (8, 8) SWCNT with two defects at different positions.

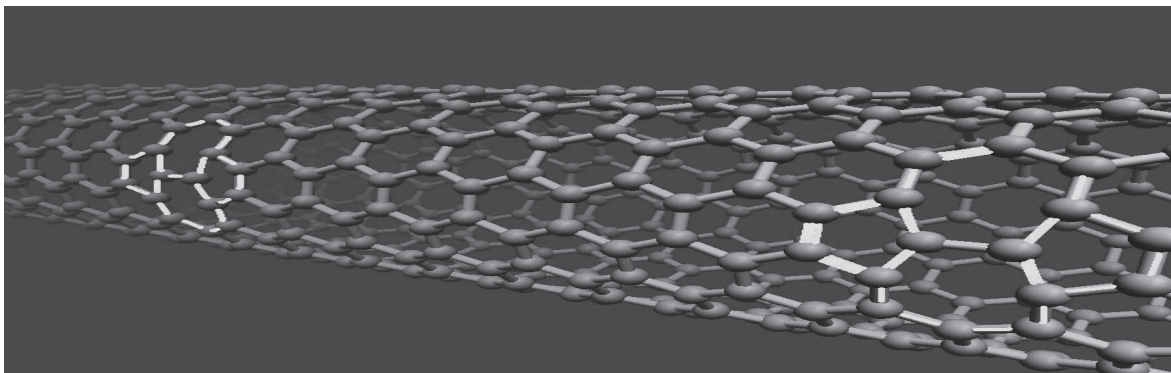


Fig. 3. Two SW-defects shown in a (8, 8) SWCNT

5.4 Variation of tube properties with defects

5.4.1 Effect of a single defect

With only one defect an SWCNT shows a scattering of data for all mechanical characteristics for different position of its formation. The variation is most pronounced for an armchair tube. Fig 4 shows the stress-strain curves for a (5, 5) SWCNT with a single defect at different positions. The curves for $z=-15$ and $z=-20$ show completely different nature. A defect at the edge which is opposite to the loading side and is oriented parallel to the axis of the tube is shown by the pink line in Fig 4. The different nature of the curve proves such defect does not affect the mechanical behavior in a considerable amount. The defect energy (E_d) for a defect near that edge ($z=15.98$ or 19.17) is greater than that of other defects for small strains but lower for large strains. While straining the tube with such defects at the far end, excess strain due to the formation of the defect is released irrespective of its orientation. However, E_d is always lower for a pristine tube compared to others at small strains but higher for large

strains. Tabulated results for the variation of the mechanical properties of the three types of tubes are given in Table 2, 3 and 4. Mechanical responses of the chiral and zigzag tubes show some variation. Maximum reduction of Young's modulus is observed with a single defect for a (5,5) tube with a defect situated near the edge and the reduction is 29%. However, the maximum reductions of Y values are 24% and 16% for a (10,0) and a (5,3) tube respectively. Ductility of a zigzag tube is not influenced by any defect present in its structure. But whatever is the position of the defect, breaking starts from the defect site. Fig 5 reveals that breaking of a chiral or armchair tube is brittle in nature. Necking is observed in case of a zigzag tube. For a pristine tube we have observed that the applied force results in many SW rotations after 10% strain as reported by Zhang et al. (Zhang et al., 1998). Stress-strain curves [Fig 4] show the variation of the mechanical behavior of the tube mainly in the non-linear portion after inclusion of a single defect at different places.

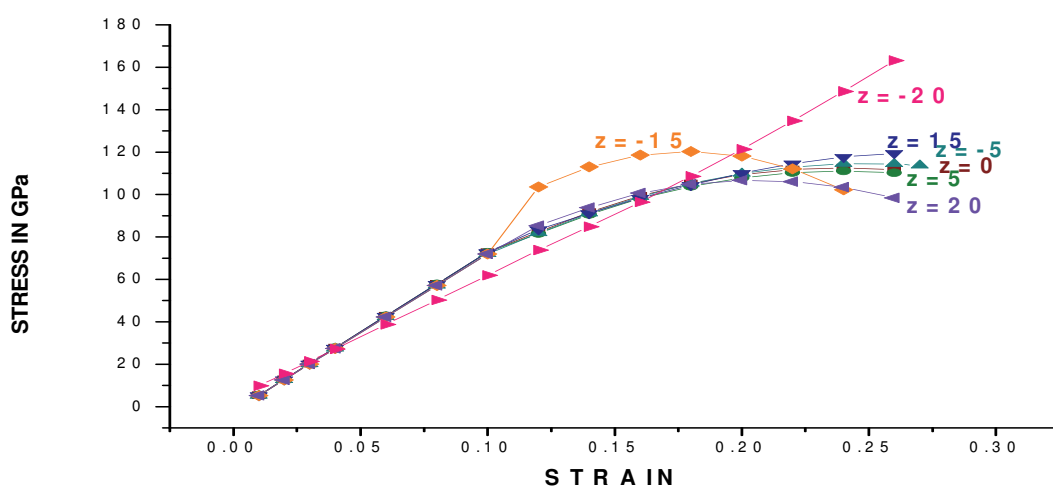


Fig. 4. Stress-strain curves for a (5, 5) SWCNT with a single defect at different positions

For a chiral tube tensile strength reduces by 34% and strain by 23% [Table 3] and the reductions are 45.6% and 25% respectively for an armchair tube [Table 4]. E_d for defects situated near the edge in case of the chiral and zigzag tubes are higher than that situated in the mid position like a zigzag tube. As the bond between two pentagons is very weak, the tube with such SW defect where pentagons oriented along the loading direction breaks easily. Where pentagons are inclined with the axis, the tube offers more resistance before breaking.

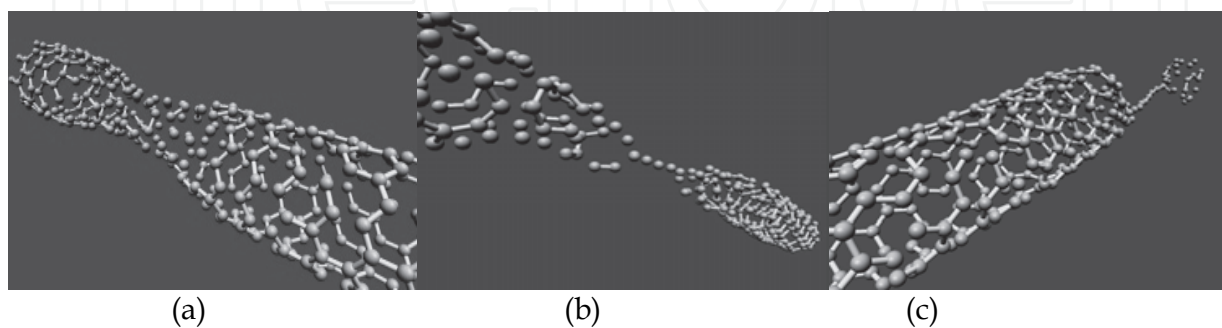


Fig. 5. Breaking patterns of a (a) (10,0) SWNT with 1 defect at (z, r, θ) position (15.98, 3.87, 9) (b) Chiral tube with a defect at (0.61, 2.65, 92) (c) armchair tube with a defect at (15.37, 3.37, 90)

5.4.2 Effect of a couple of defects

More variation of result is obtained after the inclusion of 2 defects [Fig 6]. But tensile strength and Y value are higher than the result of inclusion of one defect except for two diagonally situated defects and when the defects are situated on the same line separated by a distance. Thus for the combinations $(-1.06, 3.87, -9)$, $(1.06, 3.87, 27)$ and $(-3.19, 3.87, 27)$, $(3.19, 3.87, 27)$ the reduction of tensile strength is 41.9% and 39.4% for the $(10, 0)$ tube. When the two defects are not on the same line, rather situated opposite to each other with z position 0 and 8.52, the defects can not reduce the strength. In each case the nature of defect-defect interference is different. The stress-strain curves are shown in Fig 6 which distinguishes between different defect separation and orientation. A defect can be represented by an edge dislocation which produces gliding motion. The glide is accompanied with attachment or breaking of bonds when atoms move together and the changes are observed for the atoms in the line of glide motion. The atoms and bonds below and above the defect change. So attraction or repulsion between defects is possible according to their distance of separation and orientation (Samsonidze et al., 2002). If attraction occurs, the moving dislocations pile up such that the energy of the system slowly decreases due to the application of the external force. On the other hand any external force should bring the system to the minimum energy state easily if repulsive interaction acts between the defects. So repulsive interference occur for the above two combinations and for the defects at $(0, 3.91, 90)$ and $(8.52, 3.91, -90)$ attraction takes place. Here, the two glide motion moves opposite to each other. The orientation angle i.e. the angle between the lines joining the two pentagons of the two defects takes a major part in defect-defect correlation.

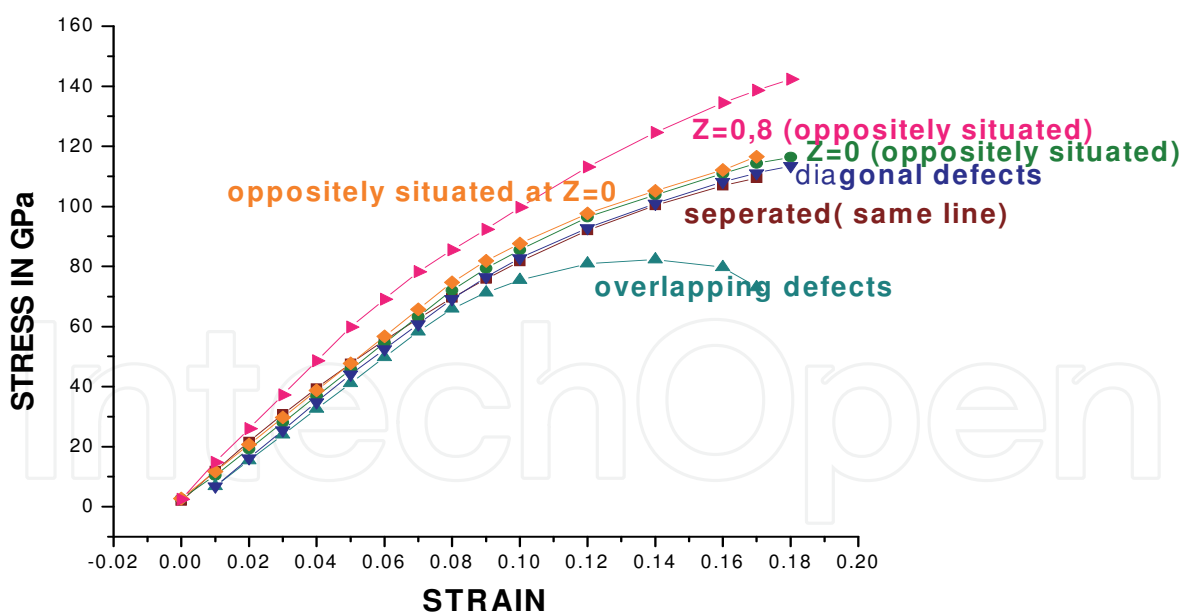


Fig. 6. Stress-strain curves for a $(10,0)$ SWCNT with 2 defects at different positions

For a chiral tube, two diagonal defects and two oppositely situated defects at the mid position reduce its strength by considerable amounts. The striking fact is that, the two overlapping defects situated side by side have no such remarkable influence on the strength. The stress-strain curves of a chiral and armchair SWCNT with 2 defects at different positions are depicted in Fig 7 and Fig 8.

Remarkable differences are observed for an armchair tube. Diagonal defects no longer change the stress-strain curve [Fig 7] compared to the defect free tube. The armchair symmetry helps attractive correlation between two diagonal defects while evidence of repulsive correlation is clear in case of the chiral tube. Repulsive correlation is much weaker for a zigzag tube in case of diagonal defects.

Breaking of a (10, 0) tube with 2 defects is accompanied with deformation of the tube in different places as shown in Fig 9(a). Other two tubes sometimes get twisted before fracture, especially for diagonal defects [Fig 9(c)]. It is surprising to note that breaking of a chiral tube [Fig 9(b)] with two defects at (4.56, 2.65, 59) and (-4.72, 2.70, 53) does not initiate from any defect site. Rather, the tube breaks at a position near the edge of the tube. The interaction of the chiral symmetry with the orientations of the defects as well as the angle between the pentagons of the defects serves a crucial role in the fracture of an SWCNT.

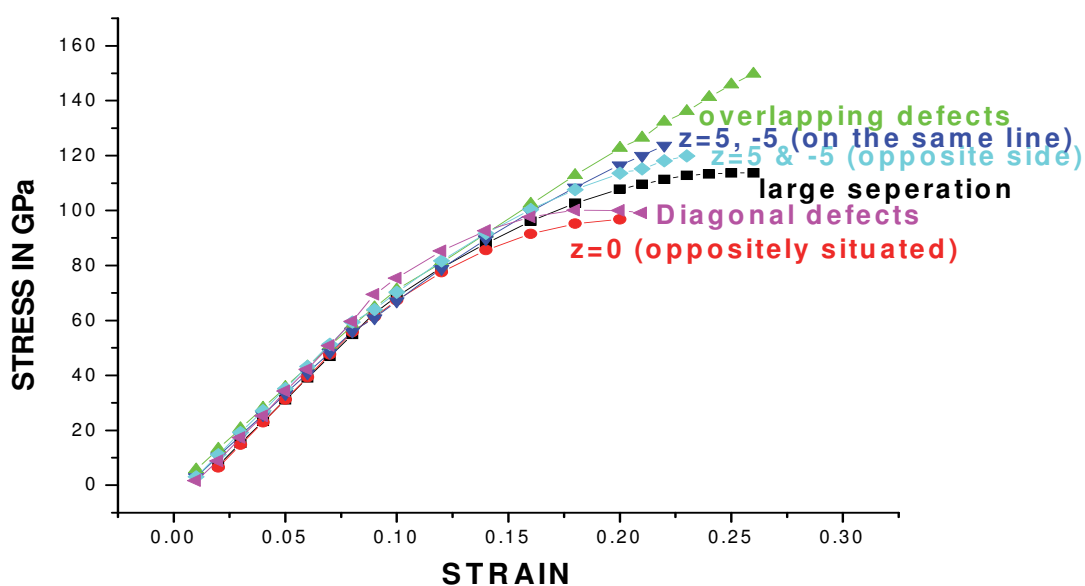


Fig. 7. Stress-strain curves of a (5, 3) SWCNT with 2 defects at different positions

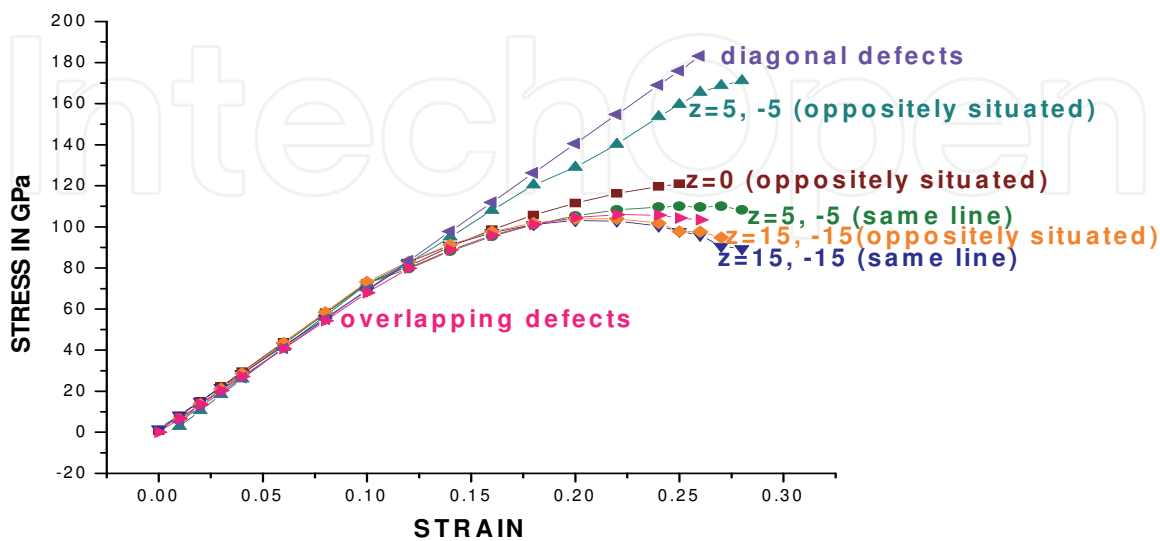


Fig. 8. Stress-strain curves of a (5, 5) SWCNT with 2 defects at different positions

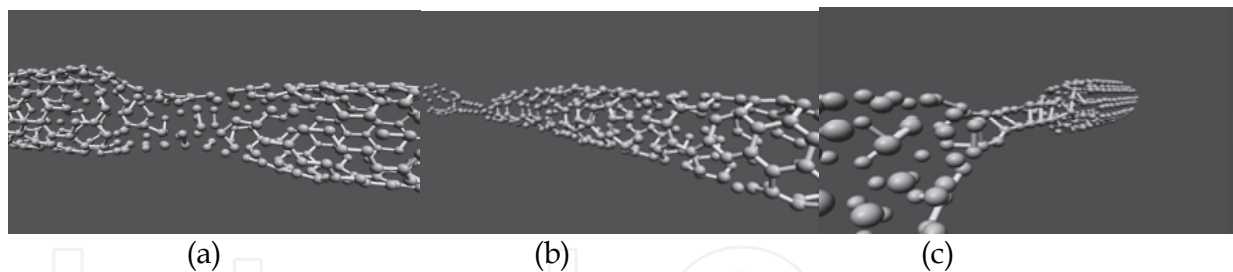


Fig. 9. Breaking of a (a) (10,0) SWCNT with two defects at (-1.06,3.87,-9) and (1.06,3.87,27) (b) (5,3) SWCNT with two defects at (4.56, 2.65, 59) and (-4.72, 2.70, 53) (c) (5,5) SWCNT with two defects at (-0.61,3.37,90) and (0.61, 3.37,126)

5.4.3 Influence of three defects

Different combinations of three defects are taken to study the effect of odd number of defects. An aggregation of three diagonal defects in a zigzag tube reduces the strength of the tube to 89.58 GPa[Fig 10]. Reduction of strength is also remarkable when the defects are close and almost on the same line (orientation of one defect differs only by 90°). Like two defects on the same line, three such defects exactly on the same line have no such pronounced effect on the tensile strength of the tube. The middle defect here is influenced complicatedly by the other two defects. In each case different results are obtained. For the defects that are oriented by some angle with respect to each other, curvature plays a significant role in decreasing the strength. For defects on the same line, mainly the separation between the defects is important. In our study maximum strain is less hampered by the inclusion of defects for a zigzag tube.

It is revealed from our study that accumulation of a number of defects has no extra influence on the mechanical response of a zigzag SWCNT. E_d increases with the increase of number of defect. But ultimately interference between defects leads to adjustment of equilibrium energy leaving some changes in stiffness and maximum tensile capacity but ultimate strain reduces only from 18% to 17% in some cases and sometimes it is fixed to 18%. The defects

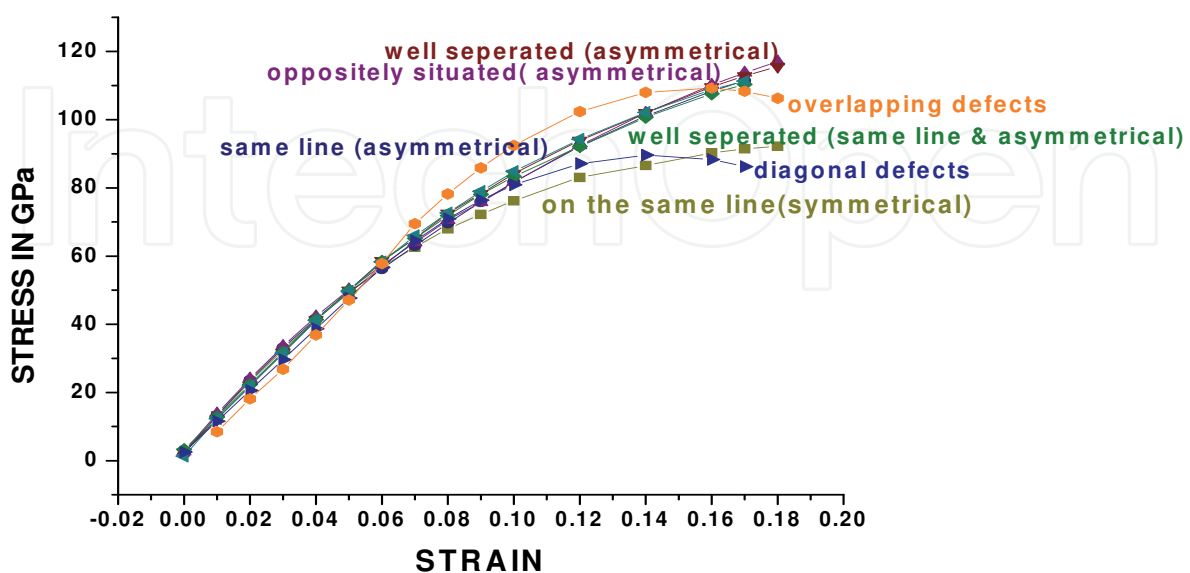


Fig. 10. Stress-strain curves for a (10, 0) SWCNT with 3 defects at different positions

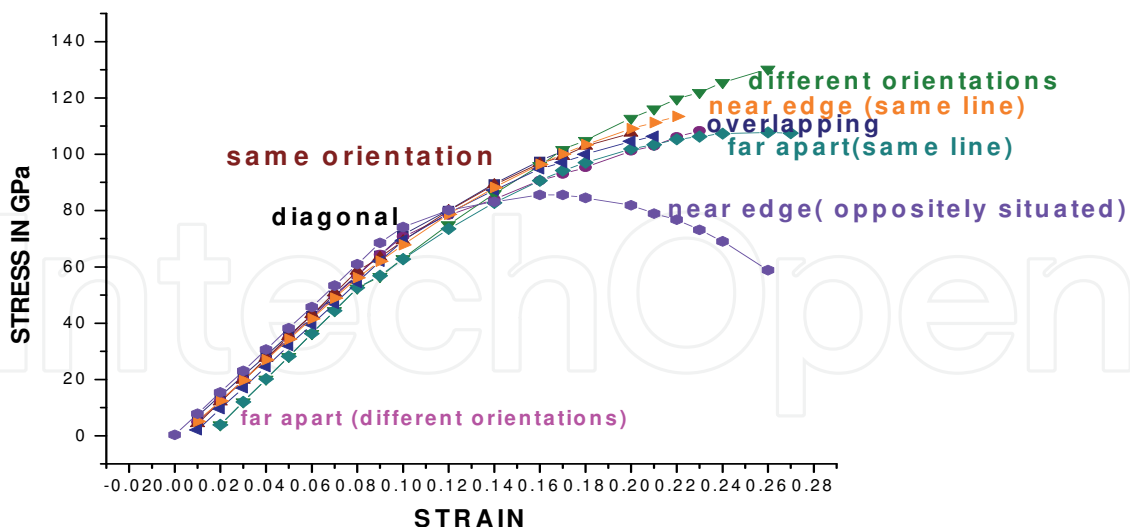


Fig. 11. Stress-strain curves for a (5, 3) SWCNT with 3 defects at different positions

created on equal distances and symmetrically on either side of the $Z=0$ position interact among themselves in such a manner that the stiffness increases than the value when the defects are asymmetric but on the same line. The observation seems to resemble with the observations of Tunvir et al. (Tunvir et al., 2008). The result of inclusion of 3 defects for a (5, 3) and (5, 5) tubes are shown in Fig 11 and 12 below. Three overlapping defects in case of a (5, 5) SWCNT change the pattern of the stress-strain curve [Fig 12] significantly. Failure stress is dropped to 85.79 GPa from 196.3 GPa and maximum strain from 32% to 26% in this case. But maximum strain is reduced mostly for 3 oppositely situated asymmetrical defects [Table 4]. In contrary, maximum stress increased to 148.2 GPa.

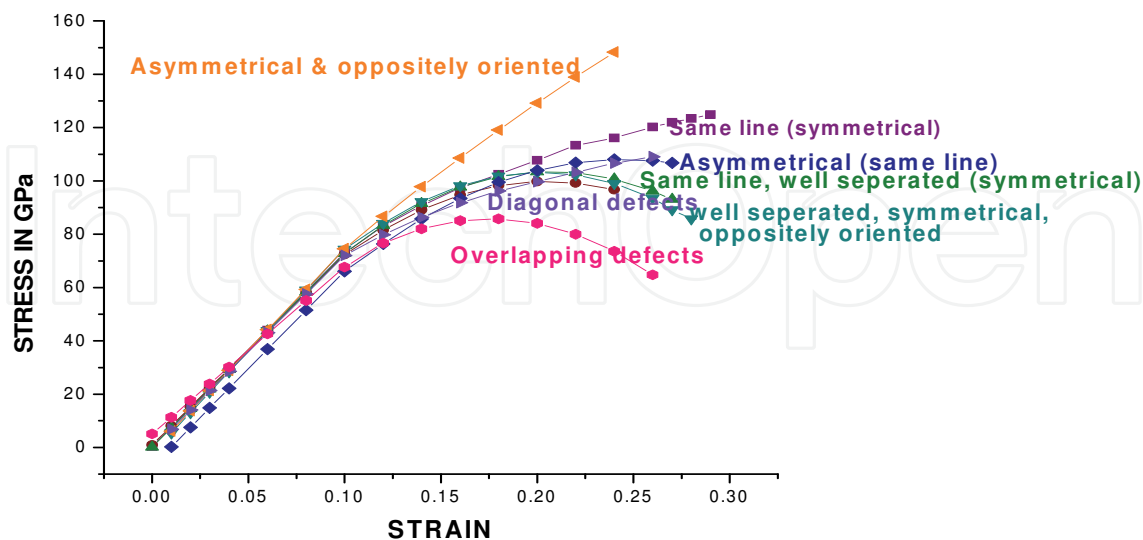


Fig. 12. Stress-strain curves for a (5, 5) SWCNT with 3 defects at different positions

Breaking of a tube with three symmetrical defects on the same line often originates from the middle defect. But sometimes, for example for 3 overlapping defects in a zigzag tube

breaking [Fig 13(a)] is not so sharp. It includes maximum bond breaking with necking. Fig 13(b) shows the fracture of a chiral tube with 3 defects while Fig 13(c) is the same picture for an armchair tube. As stated earlier, twisting of the tube in Fig 13(b) is prominent.

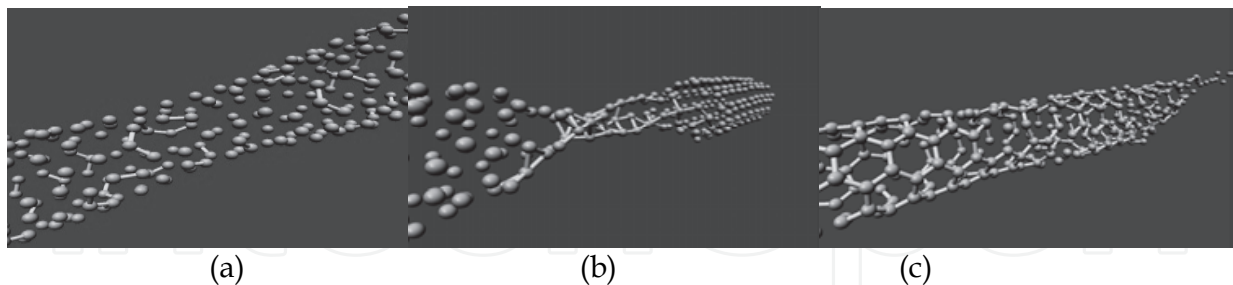


Fig. 13. Breaking of a (a) (10, 0) SWCNT with 3 defects at (0.00,3.91,90), (4.26,3.91,126), (3.91, 3.87, 171), (b) chiral SWCNT with 3 defects at (0.00,3.91,90), (-8.52,3.91,-90), (-17.04,3.89,90) and (c) an armchair SWCNT with 3 defects at (-5.53,3.37,-90),(0.61,3.37,90), (5.53,3.37,-90)

5.4.4 Results of inclusion of 4 defects at different positions

When four SW defects are introduced in the three different SWCNTs, an armchair tube is found to be influenced greatly by it [Table 4]. Tensile strain of an armchair SWCNT is dropped by 53%. The maximum strain of a chiral SWCNT [Table 3] is greatly influenced by the inclusion of 4 defects while such change is not observed for a zigzag tube [Fig 14, Table 2]. Two pairs of diagonal defects reduce the ductility of a chiral tube by 46%. 16% failure strain in this case is close to the experimental result of M. F. Yu (Yu et al, 2000c). Sharp breakings are observed for a chiral [Fig 15(b)] and an armchair [Fig 15(c)] tubes where breaking of a zigzag tube [Fig 15(a)] is not always so sharp.

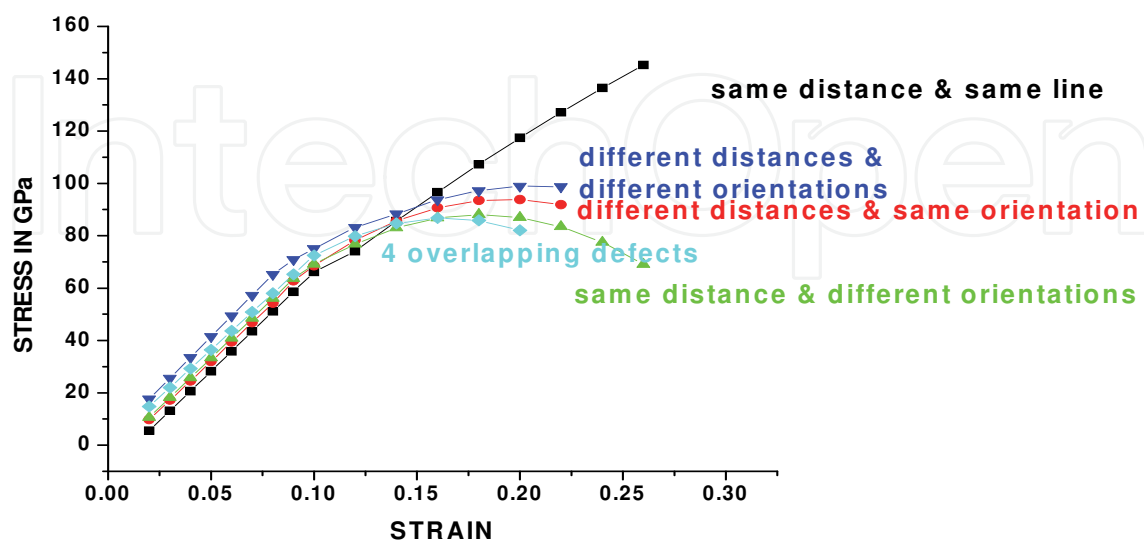


Fig. 14. Stress-Strain curves of a (10, 0) SWNT with 4 defects at different positions

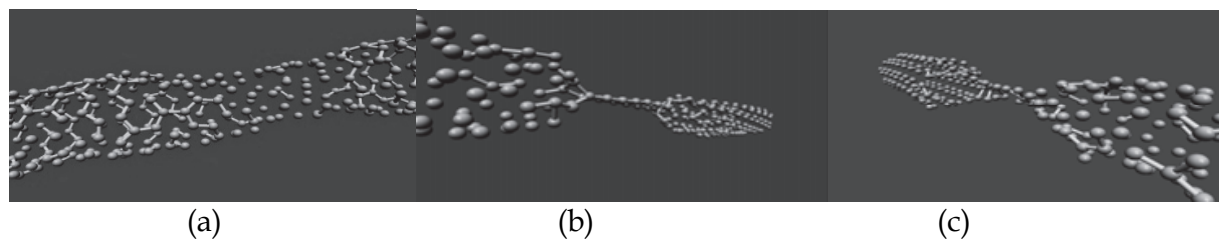


Fig. 15. Breaking of (a) a (10,0) SWCNT with 4 defects at (z, r, θ) positions $(-4.26, 3.91, 90)$, $(12.78, 3.91, 90)$, $(4.26, 3.91, 90)$, $(-12.78, 3.91, 90)$ (b) (5,3) SWCNT with 4 defects at $(-5.02, 2.73, 97)$, $(0.61, 2.65, 92)$, $(3.04, 2.65, 99)$, $(7.45, 2.70, 90)$ (c) (5,5) SWCNT with 4 defects at $(-4.3, 3.37, 90)$, $(-1.84, 3.37, 126)$, $(5.53, 3.37, 90)$ and $(6.76, 3.37, 126)$

5.4.5 Comparison between the three tubes considering the same defects inside

The difference between the mechanical responses of the three types of SWCNTs is studied and they are tabulated in Table 2, 3 and 4. When the three tubes are considered with the same defective condition, large variations are observed. For example, Fig 16 and Fig 17 are the stress strain curves of three tubes with 2 diagonal defects [Fig 16] and four symmetrical defects on the same line [Fig 17] respectively. Nature of the curves is completely changed in the two cases. That proves the symmetry dependent characteristics of single-wall carbon nanotubes when their mechanical properties are concerned. From Table 1, a summary of the results can be obtained.

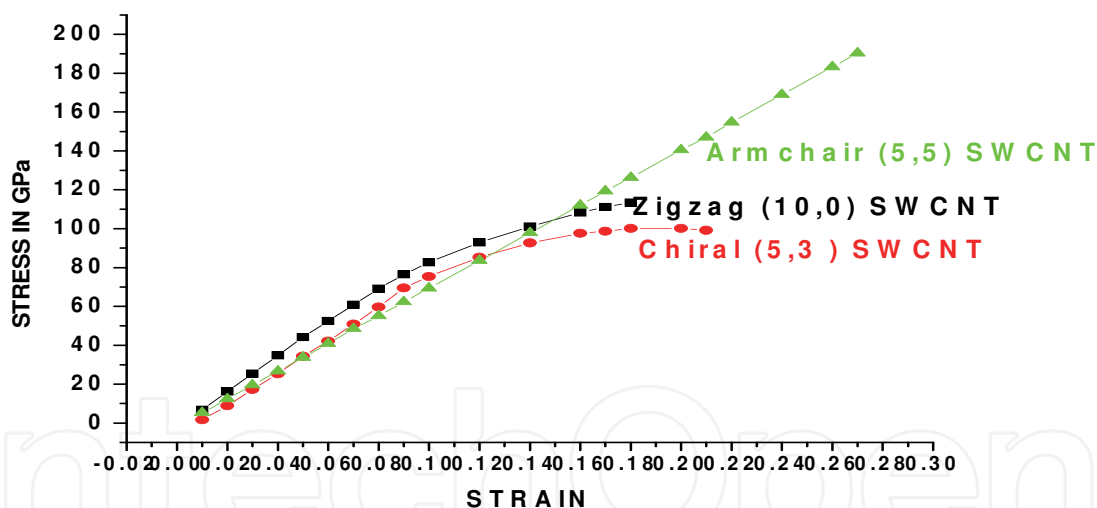


Fig. 16. Comparison of the strain-strain curves of the three tubes for 2 diagonal defects

The above study reveals that the structure of a CNT has special effect on its mechanical behavior. Zigzag symmetry has less influence on the ductility, where chiral and zigzag symmetry affect the ductility greatly. So the ductility of a zigzag SWCNT is not influenced by the presence of SW defects in its structure. A chiral tube shows less stability with increasing number of defects. Neighboring defects, especially overlapping defects reduce the strength of a zigzag and armchair tubes mostly but for chiral tube effect of overlapping defects is not so pronounced. For a cylindrical geometry of a CNT, their mechanical response is thus can be influenced by the position, arrangement and orientation of the defects as well as by the symmetry of the tube. Table 1 gives the comparison in tabulated form.

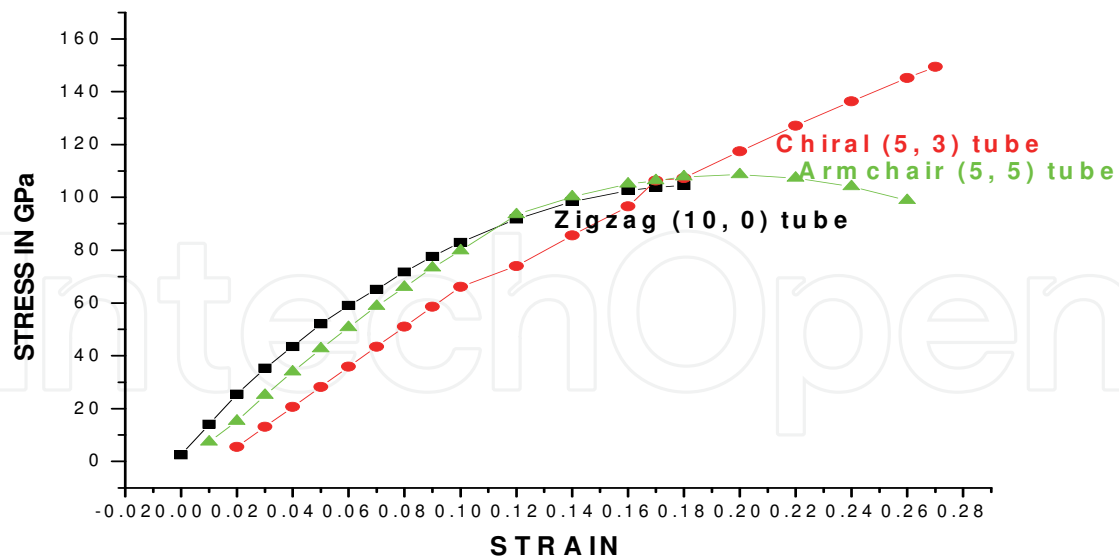


Fig. 17. Comparison of the stress-strain curves of the three tubes for 4 symmetric defects on the same line

SWCNT	Maximum reduction of γ value and (z, r, θ) position	Maximum reduction of failure stress and (z, r, θ) position	Maximum reduction of ductility and (z, r, θ) position
Zigzag: (10, 0)	23% for 4 defects at (0.00,3.91,90),(4.26,3.91,90) (-4.26,3.91,90),(7.45,3.87,99)	41.9% for 2 defects at (-1.06,3.87,-9), (1.06,3.87,27)	No significant reduction
Chiral: (5, 3)	10.4% for 3 defects at (-21.15,2.73,94), (0.61,2.65,92), (21.15,2.7,86)	42.9% for three defects at (-19.93,2.7,97), (0.46,2.73,24), (19.93,2.73,83)	46.7% for 4 defects at (-6.24, 2.7, 94),(-2.59, 2.73,105) (0.61, 2.65, 92), (3.8, 2.73, 79)
Armchair: (5, 5)	29.7% for 1 defect at (-19.06, 3.37, 36)	56.3% for three defects at (-1.84,3.37,90),(0.61,3.37,90), (3.07,3.37,90)	31.25% for 4 defects at (-4.3,3.37,90), (1.84,3.37,126) (5.53,3.37,90),(6.76,3.37,126)

Table 1. Maximum reduction of Young's modulus, failure stress and ductility for the zigzag, chiral and armchair SWCNTs and the corresponding (z, r, θ) values

Unlike the bulk materials, defects of various kinds are not always degrading the material properties, but they may also be beneficial for fixing up the point of chemical functionalization, charge injection and symmetry breaking effects and also may facilitate spectroscopic characterization process. Defect controlled future applications of CNTs have now been paid attention and efforts are made to successfully create suitable type and quantity of defects in their structure for specific purposes without compromising their other excellent properties. Production of Y or T junction for producing electronic devices or functionalization with different chemical groups at the defect sites to enhance cohesion of the CNT fibers with the matrix element are some of the common uses of defect sites.

The calculated result showing the interaction between SW defects however is still to be proved experimentally. But the sites of SW defects are used for functionalisation of chemical

	Position of defect/ defects (Z, r, θ)	Young's modulus (TPa)	Failure Stress(GPa)	Maximum Strain
Single defect:	1. (0, 3.91, 18)	0.832	105.34	17%
	2. (9.58, 3.87, 99)	0.859	104.66	18%
	3. (-9.58, 3.87, 99)	0.847	103.59	17%
	4. (15.98, 3.87, 9)	0.824	116.67	18%
	5. (-15.98, 3.87, 9)	0.846	104.14	17%
	6. (19.17, 3.91, 36)	0.821	127.71	18%
	7. (-19.17, 3.91, 36)	0.829	106.67	17%
2 defects	: 1. (-4.26,3.91,54), (4.26,3.91,54)	0.891	109.44	17%
	2. (-4.26,3.91,90), (4.26,3.91,-90)	0.873	116.38	18%
	3. (0,3.91,90), (8.52,3.91,-90)	1.00	141.7	18%
	4. (-1.06,3.87,-9), (1.06,3.87,27)	0.849	82.31	18%
	5. (2.13,3.91,0), (0.00,3.91,90)	0.893	113.5	18%
	6. (0.00,3.91,-18), (0.00,3.91,162)	0.900	116.58	18%
	7. (-3.19,3.87,27), (3.19,3.87,27)	0.832	85.87	18%
3 defects	: 1. (-4.26,3.91,99), (0.00,3.91,90), (4.26,3.91,90)	0.904	92.19	18%
	2.(0.00,3.91,90), (-4.26,3.91,90), (8.52,3.91,90)	0.865	111.41	17%
	3. (-4.26,3.91,-90), (4.26,3.91,90), (17.04,3.91,90)	0.95	117.02	18%
	4. (0.00,3.91,90), (-8.52,3.91,-90), (-17.04,3.89,90)	0.94	115.6	18%
	5. (0.00,3.91,90), (-8.52,3.91,90), (-17.04,3.91,90)	0.924	110.36	17%
	6. (0.00,3.91,90), (8.52,3.91,90), (17.04,3.91,90)	0.946	111.28	17%
	7. (0.00,3.91,90), (4.26,3.91,126), (3.91,3.87,171)	0.892	89.58	17%
	8. (0.00,3.91,90), (3.91,3.87,99), (7.45,3.87,99)	0.898	109.28	18%
4 defects	: 1. (-4.26,3.91,90), (12.78,3.91,90), (4.26,3.91,90), (-12.78,3.91,90)	0.941	104.5	18%
	2. (-4.26,3.91,90), (-12.78,3.91,90), (4.26,3.91,-90), (12.78,3.91,-90)	0.859	109.88	17%
	3. (-4.26,3.91,90), (12.78,3.91,90), (4.26,3.91,-90), (-12.78,3.91,-90)	0.868	115.5	18%
	4. (-8.52,3.91,90), (-4.26,3.91,90), (0.00,3.91,90), (4.26,3.91,90)	0.871	89.6	18%
	5. (0.00,3.91,90), (4.26,3.91,90), (-4.26,3.91,90), (7.45,3.87,99)	0.814	112.17	18%

Table 2. Mechanical behavior of a (10,0) SWCNT with one, two, three and four defects at different positions

groups, mainly carboxylic group which in turn, is exploited for better adhesion between CNT and matrix in the composite materials. Composites made up of CNT as reinforcements have many potential applications, e.g. for making of spacecrafts, sports goods etc. Y or T junctions may be prepared utilizing the presence of defects which can be used for preparing nano transistor. The functioning of those devices may be influenced by the presence of odd or even number of defects. Also, several such junctions can be produced and linked up

for building up of mesh like architectural construction. The interaction between the odd and even number of defects may be exploited to strengthen such structure. The extraordinary mechanical, electrical and thermal properties of the CNTs have been exploited in biological applications also, basically in drug delivery system.

	Position of defect/ defects (Z, r, θ)	Young's modulus (TPa)	Failure Stress(GPa)	Maximum Strain
Single defect:	1. (0.61, 2.65, 92)	0.808	133.51	24%
	2. (9.89, 2.7, 97)	0.752	115.25	23%
	3. (-9.89, 2.73, 83)	0.774	98.907	21%
	4. (14.91, 2.65, 0)	0.743	111.09	23%
	5. (-14.91, 2.65, 0)	0.81	121.41	22%
	6. (20.24, 2.7, 39)	0.78	114.57	21%
	7. (-19.63, 2.73, 53)	0.809	111.47	22%
2 defects	: 1. (-1.83, 2.65, 84), (0.61, 2.65, 92)	0.75	149.72	26%
	2. (4.56, 2.65, 59), (-4.72, 2.7, -53)	0.757	129.95	24%
	3. (5.02, 2.7, 83), (-5.02, 2.7, -83)	0.803	119.93	23%
	4. (-1.22, 2.65, -4), (1.22, 2.65, 4)	0.832	100.1	21%
	5. (-19.93, 2.7, 97), (19.93, 2.73, 83)	0.791	113.73	26%
	6. (0.61, 2.65, 92), (-0.61, 2.65, -92)	0.821	96.76	20%
3 defects	: 1. (0.46, 2.73, 24), (3.04, 2.65, 119), (5.63, 2.73, 174)	0.715	101.14	17%
	2. (-0.76, 2.7, 20), (2.89, 2.73, 31), (6.09, 2.65, 18))	0.742	108.26	23%
	3. (-5.02, 2.73, 97), (0.61, 2.65, 92), (5.02, 2.7, 83)	0.775	107.43	20%
	4. (-15.52, 2.65, 88), (0.61, 2.65, 92), (14.3, 2.65, 88)	0.809	130.23	26%
	5. (-15.52, 2.65, 88), (0.46, 2.73, 24), (15.52, 2.65, -88)	0.748	106.35	21%
	6. (-21.15, 2.73, 94), (0.61, 2.65, 92), (21.15, 2.7, 86)	0.729	113.408	22%
	7. (-19.93, 2.7, 97), (0.46, 2.73, 24), (19.93, 2.73, 83)	0.758	85.57	26%
4 defects	: 1. (-5.02, 2.73, 97), (0.61, 2.65, 92), (3.04, 2.65, 99), (7.45, 2.7, 90)	0.74	93.81	20%
	2. (-15.52, 2.65, 88), (-7.45, 2.73, 90), (7.45, 2.7, 90), (14.30, 2.65, 88)	0.758	145.22	26%
	3. (-15.52, 2.65, 88), (-5.02, 2.73, 97), (5.02, 2.73, -97), (15.52, 2.65, -88)	0.756	88.09	18%
	4. (-19.93, 2.7, 97), (-9.89, 2.73, 83), (0.00, 3.91, 90), (4.26, 3.91, 90)	0.792	98.92	20%
	5. (-6.24, 2.7, 94), (-2.59, 2.73, 105) (0.61, 2.65, 92), (3.8, 2.73, 79)	0.814	86.81	16%

Table 3. Mechanical behavior of a (5, 3) SWCNT with one, two, three and four defects at different positions

For hydrogen storage, the defect sites are responsible for better absorption. The interaction between defects should be studied for the full exploitation of CNT properties, particularly in composite materials for achieving the target of their possessing very high strength. While functionalizing a CNT for making composite materials, the reduction of the strength of the CNT due to defect-defect interaction may be controlled by functionalizing the CNTs at proper defect positions.

Not only the number of defects, but their position and orientation are also important while analyzing their effects on the mechanical properties of the carbon nanotubes. This dependence varies with the symmetry of the tubes. Young's modulus of a zigzag tube with four defects placed symmetrically almost on the same line is reduced largely compared to a defect free tube. Two diagonal and overlapping defects are found to have maximum reducing effect on failure stress for the tube. The ductility of a zigzag tube is almost insensitive to the presence of defects in its structure.

For a chiral tube, the maximum reduction of Y value is noticed for three well separated symmetrically situated defects. The failure stress of a chiral tube is mostly influenced by three well separated defects (symmetrically situated around $z=0$ position). 46.7% reduction of failure strain is calculated for a chiral tube with four defects for some specific combinations. For an armchair tube reduction of Y value is maximum for 1 defect near the edge. 56.3% reduction of strength is reported for the tube with three defects on the same line but asymmetrically placed about $z=0$. 31.25% reduction of failure strain is reported for an armchair tube with four defects for some specific combinations.

There are many possibilities of the arrangement of different number of defects due to which the strength and stiffness of the CNTs may vary differently. In our investigation, we have observed the variation of these mechanical properties (strength and stiffness) for several combinations of separating distances as well as different orientations of the defects in the structure of the CNTs. In some cases, the reduction of these major properties is significant whereas in some other cases it is less. Now, if we can functionalize the CNTs at those defect sites where, the reduction of their strength or stiffness is negligible, then it may be possible to fabricate composite materials with such functionalized CNTs without losing their strength or stiffness much. For example, for two SW defects at (z, r, θ) positions of $(0, 3.91, 90)$ and $(8.52, 3.91, -90)$, the reduction of both the strength and stiffness of the zigzag SWCNT $(10, 0)$ is minimum. So, functionalizing the tube at those defect sites will not reduce much of the strength of the composite material reinforced by them. Development of better experimental technique to identify the suitable sites of defects for functionalization will help the composite builders in this respect in near future.

6. Variation of mechanical properties and fracture behavior of single wall carbon nanotubes on bundle formation

Using the 2nd generation REBO potential with smoothing at cut-off region, MD simulation is carried out for three different types of tubes. Then bundle of each type is taken containing three of them in each bundle and then one bundle of the mixture of the three types is taken and simulated separately. Lengths of the single zigzag, armchair and chiral tubes are 85.18 Å, 98.58 Å, 119.26 Å respectively. As before, room temperature is maintained by Berendsen thermostat. By stretching the tubes in small strain increments, the equilibrium potential energy is calculated by simulation. Keeping one end fixed the other end of the bundle is stretched gradually from the unstretched condition in such a way that all the tubes are

	Position of defect/ defects (Z, r, θ)	Young's modulus (TPa)	Failure Stress(GPa)	Maximum Strain
Single defect:	1. (0.61, 23.37, 90)	0.749	112.56	26%
	2. (5.53, 3.37, 90)	0.749	111.05	26%
	3. (-5.53, 3.37, 90)	0.741	141.42	27%
	4. (15.37, 3.37, 90)	0.749	119.44	26%
	5. (-15.37, 3.37, 90)	0.741	120.26	24%
	6. (19.06, 3.37, 90)	0.741	106.72	28%
	7. (-19.06, 3.37, 36)	0.572	178.16	28%
2 defects	: 1. (0.61, 3.37, 90), (0.61, 3.37, -90)	0.717	120.97	25%
	2. (-5.53, 3.37, 90), (5.53, 3.37, 90)	0.74	109.67	28%
	3. (-5.53, 3.37, 90), (5.53, 3.37, -90)	0.77	190.38	30%
	4. (-15.37, 3.37, 90), (15.37, 3.37, 90)	0.672	103.09	20%
	5. (-15.37, 3.37, 90), (15.37, 3.37, -90)	0.744	103.97	27%
	6. (-0.61, 3.37, 90), (0.61, 3.37, 126)	0.711	190.32	27%
	7. (-0.61, 3.37, 90), (1.84, 3.37, 90)	0.678	106.01	26%
3 defects	: 1. (-5.53, 3.37, 90), (0.61, 3.37, 90), (5.53, 3.37, 90)	0.726	124.83	29%
	2. (-5.53, 3.37, -90), (0.61, 3.37, 90), (5.53, 3.37, -90)	0.714	99.78	24%
	3. (-20.29, 3.37, 90), (0.61, 3.37, 90), (20.29, 3.37, 90)	0.726	103.42	27%
	4. (-20.29, 3.37, -90), (0.61, 3.37, 90), (20.29, 3.37, -90)	0.766	103.18	28%
	5. (0.61, 3.37, 90), (6.76, 3.37, 90), (15.37, 3.37, 90)	0.732	108	27%
	6. (0.61, 3.37, 90), (6.67, 3.37, -90), (15.37, 3.37, -90)	0.76	148.3	24%
	7. (-1.84, 3.37, 90), (-0.61, 3.37, 126), (1.84, 3.37, 162)	0.724	109.02	26%
	8. (-1.84, 3.37, 90), (0.61, 3.37, 90), (3.07, 3.37, 90)	0.625	85.79	26%
4 defects	: 1. (-11.68, 3.37, 90), (-4.3, 3.37, 90), (4.3, 3.37, 90), (11.68, 3.37, 90)	0.813	108.57	26%
	2. (-11.68, 3.37, -90), (-4.3, 3.37, -90), (4.3, 3.37, 90), (11.68, 3.37, 90)	0.764	98.54	26%
	3. (-11.68, 3.37, -90), (4.3, 3.37, -90), (-4.3, 3.37, 90), (11.68, 3.37, 90)	0.679	92.82	26%
	4. (-4.3, 3.37, 90), (-1.84, 3.37, 126), (5.53, 3.37, 90), (6.76, 3.37, 126)	0.706	91.09	22%
	5. (-1.84, 3.37, 90), (0.61, 3.37, 90), (4.3, 3.37, 90), (6.76, 3.37, 90)	0.773	113.12	26%

Table 4. Mechanical behavior of a (5, 5) SWCNT with one, two, three and four defects at different positions

stretched equally. Intertube interaction is modeled with Lennard-Jones potential. For a SWCNT bundle, volume of each tube is calculated separately and then added to get the total volume.

6.1 Mechanical characteristics of isolated tubes

A zigzag SWCNT exhibits a high Young's modulus value of 1.47 TPa with 16% ductility. Calculated failure stress is 76.77 GPa. Stress strain curves of the three tubes are shown in Fig 8.1. For the (5, 0) tube, stress increases slowly upto 8% more or less linearly and then flattens giving a yield point near 9% strain. On straining the tube beyond 12% strain for a zigzag SWCNT, as reported by Zhang et al. (Zhang et al., 1998), we have observed SW rotation that ultimately leads to rupture of the tube. After 18% strain, the tube breaks totally with the formation of a series of SW rotations. The stress strain curves of isolated (5, 5) and (5, 3) tubes [Fig 18] are somewhat different in nature. Also their failure stress and failure strain values are different. The single (5, 5) tube has the highest fracture strain of 26% compared to the other two. Table 5 gives the detailed picture of the failure stress and strain values. However, the chiral SWCNT shows the maximum breaking stress of 115.65 GPa.

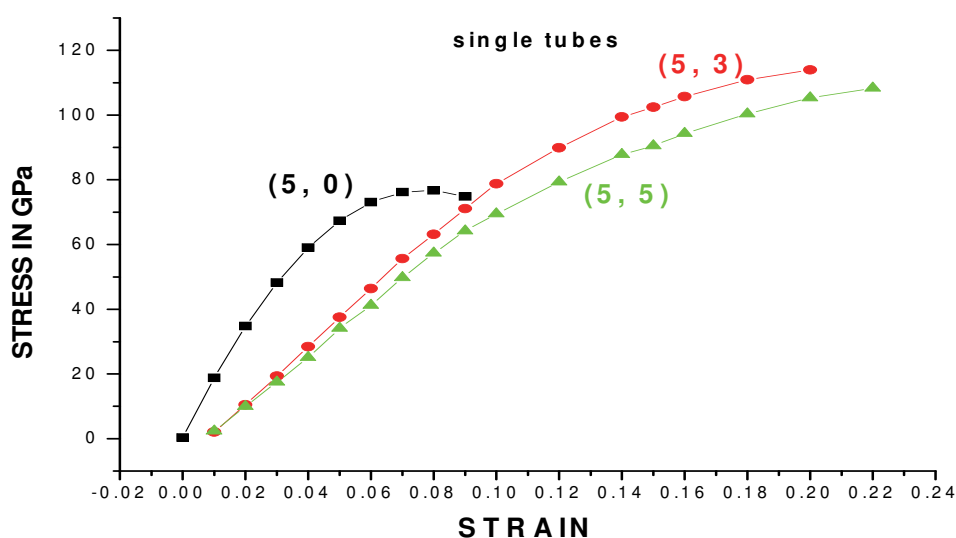


Fig. 18. Stress-strain curves of three different types of isolated tubes.

Young's modulus values agree very well with the experimental data of Krishnan et al. (Krishnan et al. 1998) Wong et al. (Wong et al., 1997), and Treacy et al. (Treacy et al., 1996). Failure stress or strain of the single tubes does not match with the experimental findings of Yu et al. (Yu et al., 2000c) which, we will show in the next part of this section, match with experiment when mixture of bundles of nanotubes are formed. Yu et al. (Yu et al., 2000c) observed 10-13% maximum strain for SWCNT bundle with failure stress varying in between 13- 52 GPa. For single tubes, our calculated values of failure stress matches with Mielke et al (Mielke, 2004) and Troya et al. (Troya, 2003) with the same potential.

Failure of these tubes [Fig 19] does not show complete rupture of the tubes. Rather they exhibit breaking of bonds all over the tubes at the breaking point.

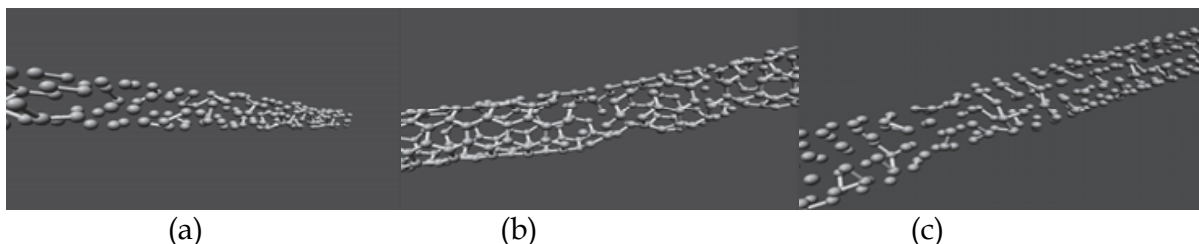


Fig. 19. Breaking patterns of an isolated (a) zigzag (b) chiral (c) armchair SWCNT

6.2 Characteristics of a bundle of three different types of SWCNTs

Single-wall carbon nanotubes that are grown by laser ablation, (Eklund et al., 2002; Guo et al., 1995; Thess et al., 1996;) arc discharge (Bethune et al., 1993; Ebbesen & Ajayan, 1992; Iijima, 1991) or the most recent HiPCO method always occur in bundles. These bundles are held together by weak interactions between the tubes. The bundles of SWCNTs are different from the isolated tubes in two respects. A bundle contains nanotubes of different chirality and slightly different diameters (Henrard et al., 2000). Bundling also changes their properties by tube interaction. Surprisingly, Young's modulus is noticeably increased to 1.60 TPa again and failure strain is reduced to 9% [Fig 20]. Failure stress is also reduced much giving a value of 68.50 GPa. Fracture of a SWCNT bundle with three (5, 3) chiral tubes is depicted in Fig 21 which are very much different in nature from the stress-strain curves of isolated tubes [Fig 19]. Table 5 shows the results in tabulated form.

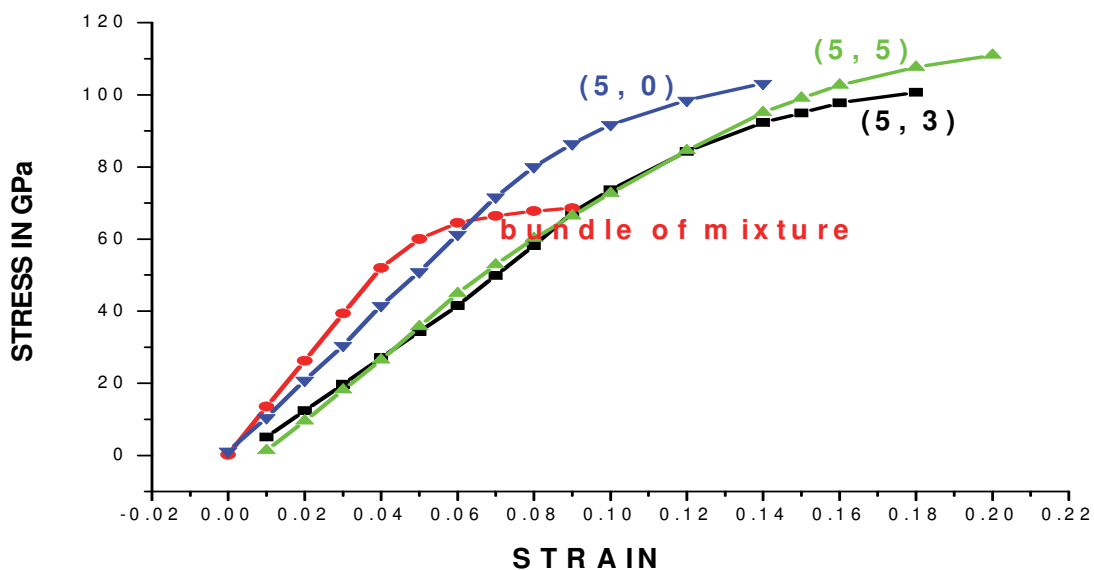


Fig. 20. Stress-strain curves of bundles of different SWCNTs

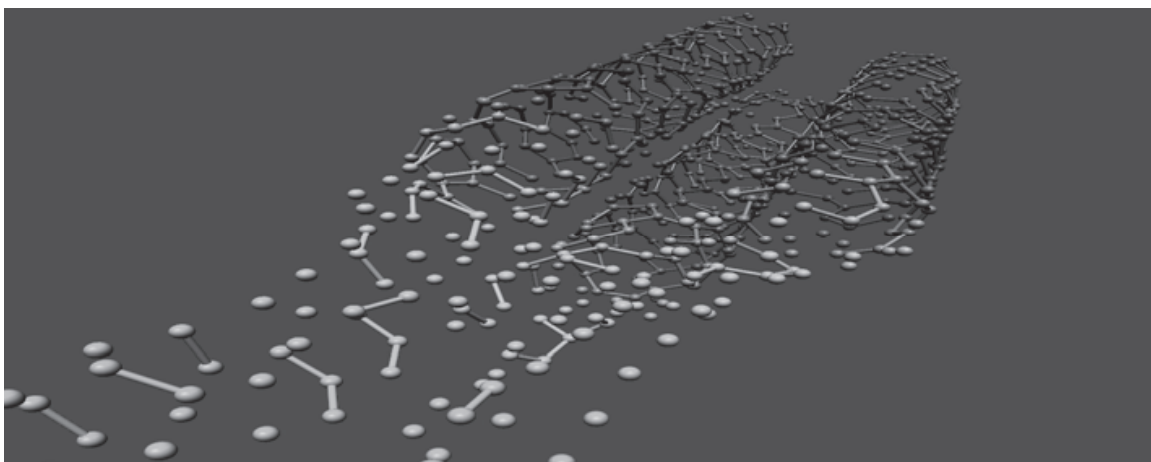


Fig. 21. Failure of a bundle of three (5, 3) SWCNTs

This changed behavior may be explained by overlapping of energy bands in nanotube bundles. Scanning tunneling spectroscopy (Wildoer et al., 1998), resonant Raman scattering (Jorio et al., 2001) and optical absorption or emission measurements (Connell et al., 2002)

confirmed the electronic DOS in carbon nanotubes. Ouyang et al (Ouyang et al., 2001) experimentally found a pronounced dip in the electronic DOS of a (8, 8) SWCNT at Fermi level inside a bundle, compared to an isolated tube. This is due to symmetry breaking by other tubes in proximity. Not always a gap is produced, but gap may also be closed for such a tube. Closing of band gap is observed for a (10, 0) tube in a bundle in (Reich et al., 2002). Due to this type of overlapping of electronic bands, attraction or repulsion arises inside the SWCNT bundle. All intermolecular/van der Waals forces are anisotropic which means that they depend on the relative orientation of the molecules. The induction and dispersion interactions are always attractive, irrespective of orientation, but the electrostatic interaction changes sign upon rotation of the molecules. That is, the electrostatic force can be attractive or repulsive, depending on the mutual orientation of the molecules giving rise to different interaction between the tubes of a bundle.

In the low energy part of the band structure the bundling of the nanotubes changes the electronic properties by symmetry breaking and by the intratube dispersion perpendicular to K_z . That also holds good for larger electronic energies also. Again, when isolated tubes of different symmetries are present, energy bands are strongly split. Reich et al. (Reich et al., 2002) showed that in a high symmetry packing of (6, 6) nanotube the degenerate bands of isolated tube remained degenerate by symmetry in the crystal. In their study, it was also revealed that the dispersion of the electronic bands perpendicular to k_z is less in a zigzag (10, 0) tubes than a (6, 6) tubes. The first two valance states at the Γ point of the brillouin zone results in a strong dispersion in the corresponding states perpendicular to k_z for armchair tubes. Chiral tubes are likely to be more complicatedly influenced by symmetry breaking and band splitting. The change of behavior of the curves for an isolated tube and their bundles can thus be explained by the change of DOS which must be taken into account while comparing a theoretical result with the experimental findings.

SWCNT	Young's Modulus (TPa)	Failure stress (GPa)	Failure strain
Zigzag (5,0)			
Single:	1.468	76.770	14%
Bundle:	1.013	105.008	15%
Armchair (5,5)			
Single:	0.792	107.913	26%
Bundle :	0.867	112.032	21%
Chiral (5,3)			
Single:	0.831	115.652	22%
Bundle:	0.729	101.017	18%
Mixture of three Different tubes	1.602	68.500	9%

Table 5. Young's modulus, tensile strength and ductility of different SWCNT types and their bundles

6.3 Effect of the number of tubes in the SWCNT bundle on their mechanical behavior

We have investigated the influence of an increasing number of tubes in an armchair (5, 5) single-wall carbon nanotube bundle on their mechanical properties under tensile and

compressive loading by molecular dynamics simulation. 2nd generation Brenner bond order potential is adopted for energy minimization in the simulation process.

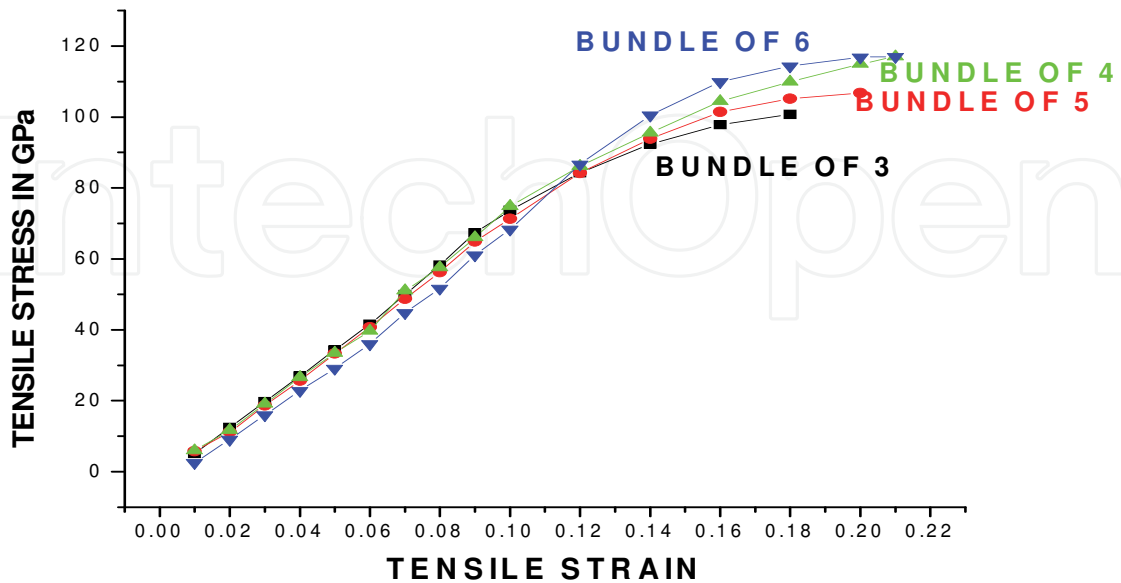


Fig. 22. Tensile stress vs. strain curves of bundles of (5, 5) SWCNTs with different number of tubes

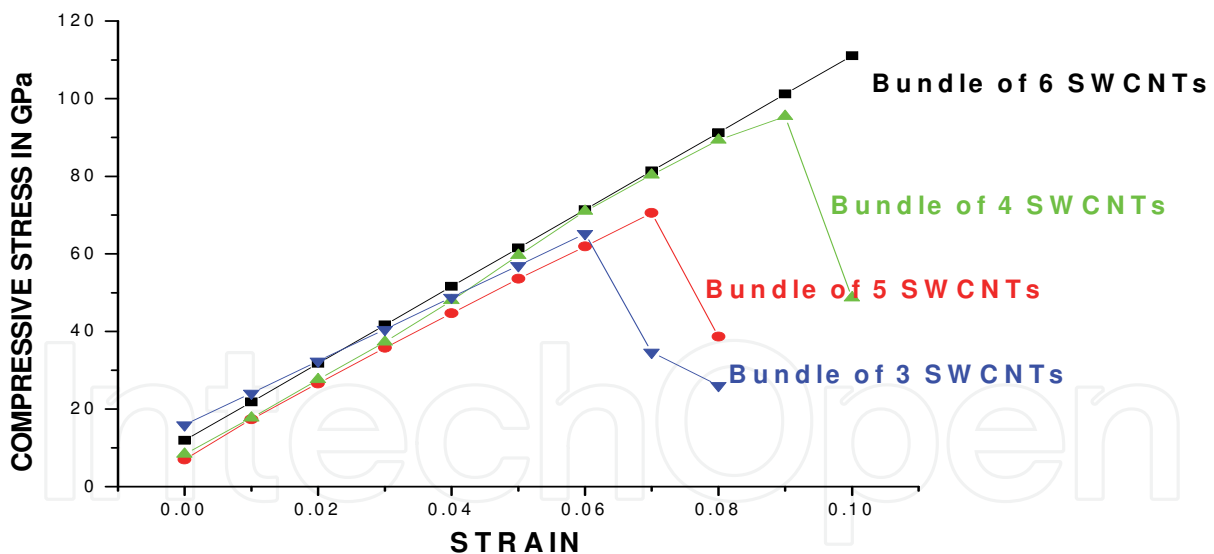


Fig. 23. Compressive stress vs. strain curves of bundles of (5, 5) SWCNTs with different number of tubes

From the stress-strain curves of the bundles [Fig 22 and 23] it can be inferred that with the increase of the number of tubes in the bundle, the bundle becomes more stiff and strong. Resemblance of the curves is noticed for 4 and 6 membered bundles in Fig 8.9. The same Figure also shows the resemblance of the curves for 3 and 5 membered bundles. The Young's modulus decreases while the compressive modulus increases with the number of tubes in a bundle [Fig 24]. But, overall increase of tensile and compressive stress [Fig 25] is

reported in this study. The maximum Young's modulus of 0.73 TPa and maximum compressive modulus of 1.00 TPa are obtained in our calculation for a bundle of three tubes. These are within the range of the experimental findings of Yu et al. (Yu et al., 2000c) and Treacy et al. (Treacy, 1996) Failure strength of about 100 GPa can be matched with the observations by Demczyk et al. (Demczyk et al., 2002) Ductility, tensile and compressive strengths agree well with the experimental results as well as with other MD simulation calculations.

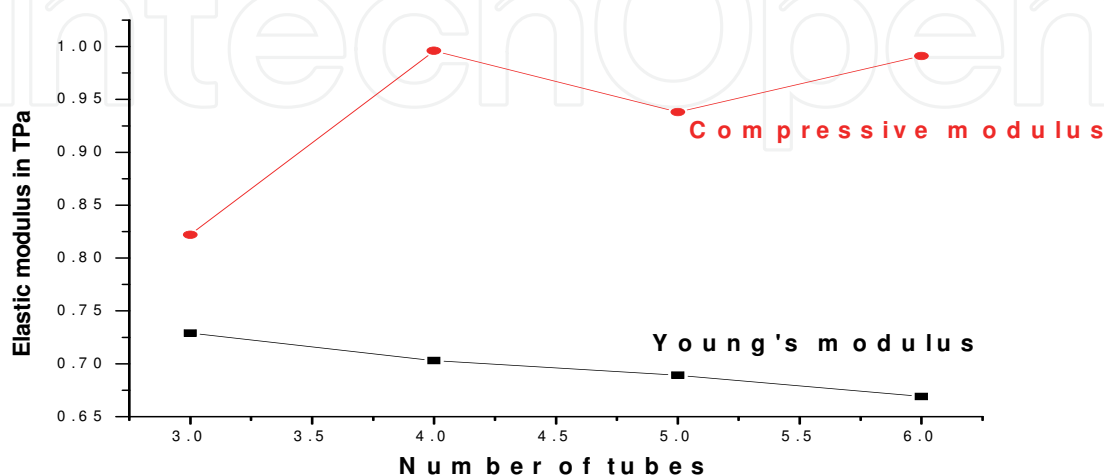


Fig. 24. The variation of elastic moduli with the number of tubes in a bundle

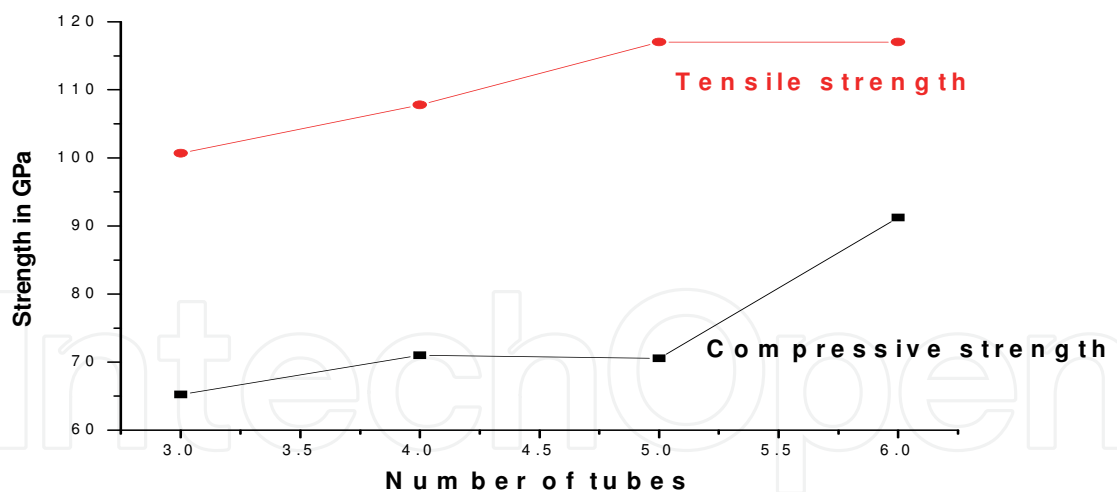


Fig. 25. The variation of strength with the number of tubes in a bundle

When the fracture of these bundles is modeled, it is observed that the bundle consisting of a fewer number of tubes breaks completely at the maximum stain value where all of its members break equally. On the other hand, only one or two tubes of a bundle with a larger number of tubes break completely at the same strain value. Compression produces kinks in the structure of the SWCNT bundles. They show complete collapse from the position of kink formation at a certain strain. The cross section of the tubes in a bundle of the carbon nanotube changes on the application of force from circular to oblate and more deformed

shape appears on the increase of strain. The breaking and buckling of the bundles are depicted in Fig 26 (a-j).

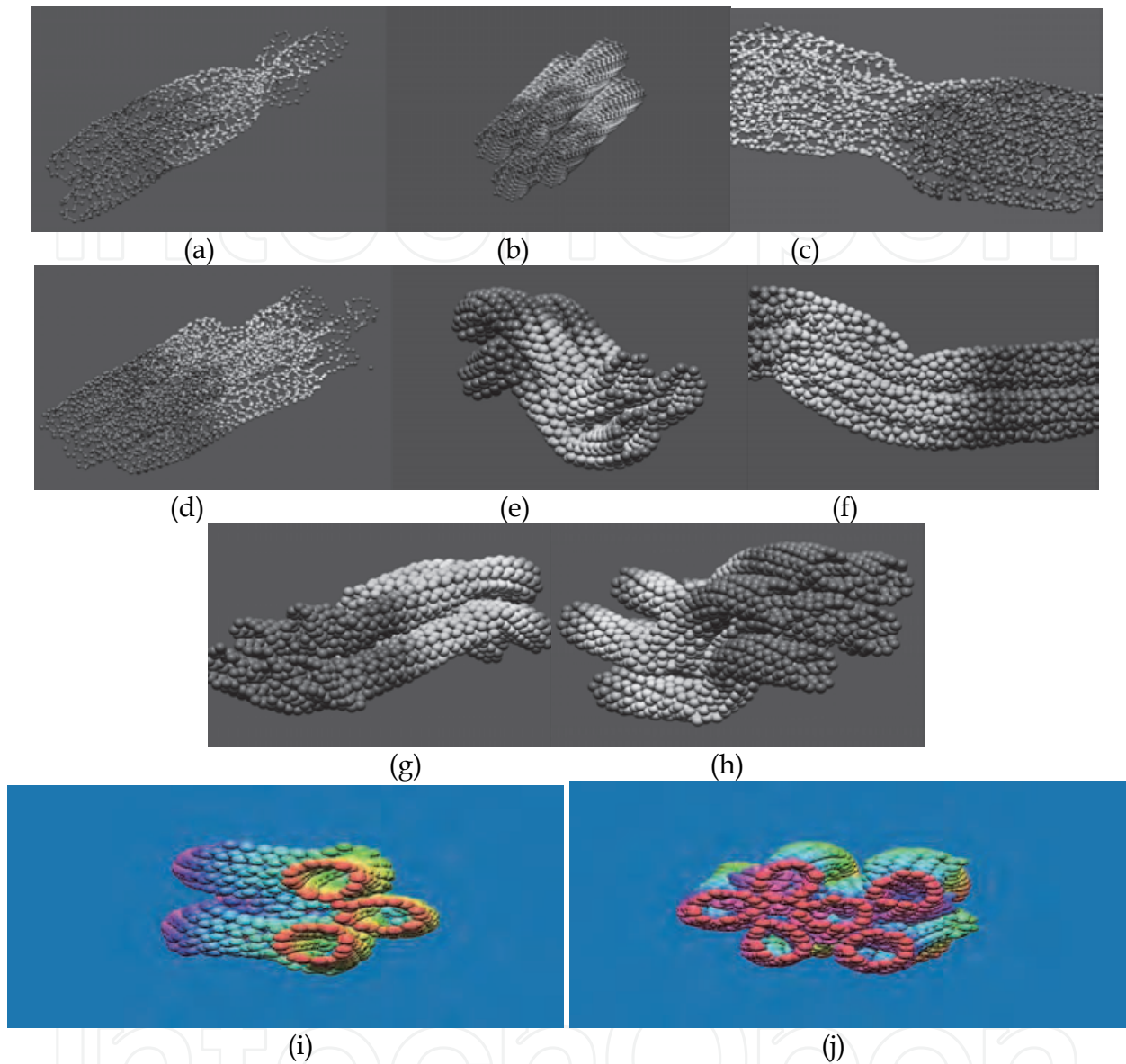


Fig. 26. **(a)** Breaking of a 3 membered bundle **(b)** A bundle of 4 tubes **(c)** breaking of a 5 membered bundle. It breaks from the middle portion. **(d)** A six membered bundle breaks near the end (not all the tubes are broken at a time) **(e)** buckling of a bundle of 3 tubes **(f)** buckling with 4 tubes **(g)** buckling with 5 tubes (tubes are distorted near the loading edge) **(h)** buckling of a six membered bundle **(i)** Distortion of the cross section of the tubes in a bundle of three SWCNTs under pressure. **(j)** Distortion of the cross section is more for a bundle of five SWCNTs. Different cross-sectional changes are observed for different tubes in the same bundle

Comparing the MD simulation results of different SWCNTs and their bundles, it can be concluded that a major reason of non-compatibility of the theoretical results with the experimentally obtained low values of failure strain and failure stress is the existence of the SWCNTs in the form of bundles where different types of tubes may be present. While

forming the bundles, the zigzag tube resists the external force strongly and the armchair tube breaks symmetrically on the application of the tensile force. 25% reduction of maximum strain is observed for a bundle of three chiral SWCNTs compared to a single tube. The reduction is maximum for a bundle of the mixture of three types and we get 43.75% decrease of the strain from the lowest strain of 16% for a single zigzag tube. Overlapping of density of states is responsible for the changed behavior of the bundle of nanotubes. Also the number of tubes in a SWCNT bundle affects their mechanical properties in a great extent.

7. Dependence of the mechanical properties of SWCNTs on the choice of interatomic potential functions

The choice of potential function in explaining the mechanical properties of CNTs is a vital factor. In Fig 1, we have already shown the stress-strain curves of three different types of defect-free SWCNTs with 2nd generation REBO potential. An armchair (5, 5), a chiral (5, 3) and a zigzag (5, 0) SWCNT exhibit stress-strain curves as shown in Fig 27 with tight binding potential. In a (5, 0) SWCNT the plastic flow region contains a plateau after which, the stress increases to 161.00 GPa. The armchair and the chiral tubes show lesser tensile strength of 141.52 GPa and 125.61 GPa respectively. But their failure strain values are same as 26%. In tight binding approximation, the (5, 5) and the (5, 3) tubes show some ductility before failure.

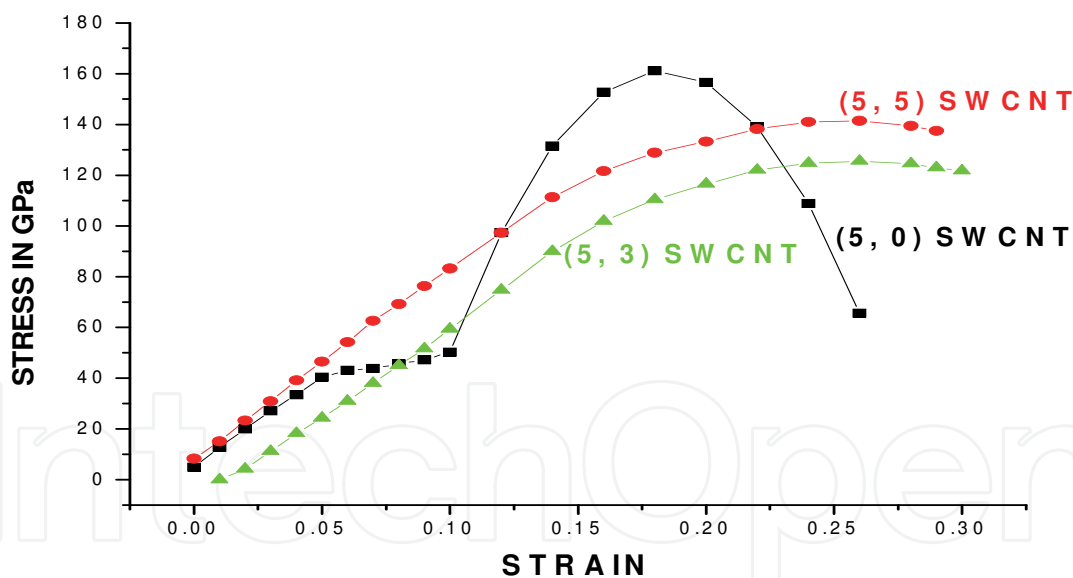


Fig. 27. Stress-strain curves of three different types of SWCNTs with tight binding potential

For three different types of defect-free tubes, the mechanical characteristics are tabulated below (Table 6). Results for the smoothed off REBO potential are taken from Fig 18.

From Table 5, we can conclude that reasonable results are obtained for REBO potential with smoothed off cut-off function. For the (5, 0) tube failure strength of 76.77 GPa and failure strain of 14% are much less than the values with other potentials. Other tubes also show much lower values of the mechanical characteristics with the former potential with respect to the others. So, the 2nd generation REBO potential with smoothed off cut-off function gives

more reasonable values with respect to the experimental values (Yu et al., 2000c). The discrepancies, still present may be due to the availability of the experimental samples in the form of bundles or due to the presence of defects in the samples.

SWCNT	Tight Binding			2 nd generation REBO			Smoothed off REBO		
	Y.M. (TPa)	F.S. (GPa)	F.Sr.	Y.M. (TPa)	F.S. (GPa)	F.Sr.	Y.M. (TPa)	F.S. (GPa)	F.Sr.
(5, 0)	1.13	161.00	18%	1.44	144.70	20%	1.47	76.77	14%
(5, 5)	0.81	141.52	26%	0.81	196.30	32%	0.79	107.91	26%
(5, 3)	1.00	125.61	26%	0.89	149.88	30%	0.83	115.65	22%

Table 6. Comparison of the results obtained for three different potentials for defect-free tubes

8. Conclusions

The dependence of mechanical properties of SWCNTs on various factors is discussed in this chapter. So by the quantitative investigation it can be concluded that for engineering interest, the mechanical properties of the CNTs can be tailored by introducing suitable number of defects in suitable positions and orientations. In the present situation, the designing of composites with desired properties is a challenging job which depends on more understanding of the properties of these reinforcing agents.

A striking change in the mechanical properties of a SWCNT is noticed when some of them form a bundle. Though we have obtained the Young's modulus and failure stress values in the experimentally specified range, the failure strain is higher than that of the experimental values for a single tube. An armchair, a zigzag and a chiral SWCNTs show higher failure strain than their bundles. Due to the overlapping of density of states a bundle of their mixture shows a drastic reduction of the failure strain (from 18% for a defect-free tube to 9% on bundle formation). Repulsive interaction between these tubes is observed in this study. Breaking of symmetry of a tube in proximity of the others is the possible reason of such changes. When we increased the number of tubes in a bundle of an armchair SWCNT, the bundle becomes stronger and stiffer. With more tubes, a bundle possesses high buckling strength also. The cross section of the tubes in a bundle deform under pressure. The cross section changes from circular to oval under the application of pressure. More deformation is observed with the increase of compressive force.

We have tried to increase the acceptability of the results obtained in the simulation procedure by choosing different potentials, in particular the Tersoff-Brenner potential and tight binding potential. Tight binding potential is used as it is.

But we have carried out simulation with 2nd generation REBO potential and also with smoothed off 2nd generation REBO potential to avoid the sudden hike of energy near the cut-off region. More reasonable results are obtained for a smoothed-off REBO potential at the cut-off region.

9. References

- Ajayan, P. M.; Ravikumar, V. & Charlier, J.-C. (1998). Surface Reconstructions and Dimensional Changes in Single-Walled Carbon Nanotubes. *Physical Review Letters*, vol. 81, No. 7, pp. 1437-1440, ISSN 0031-9007
- Alder, B.J. & Wainwright, T.E. (1957). Phase Transition for a Hard Sphere System. *Journal of Chemical Physics*, vol. 27, No. 5, pp. 1208-1209, ISSN 0021-9606
- Alder, B.J. & Wainwright, T.E. (1959). Studies in Molecular Dynamics. I. General Method. *Journal of Chemical Physics*, vol. 31, No. 2, pp. 459-466, ISSN 0021-9606
- Allen, M.P. & Tildesly, D.J. (1989). *Computer Simulation of Liquids*. Oxford University press, ISBN 0 19 855645, Oxford, New York
- Andrews, R.; Jacques, D.; Rao, A.M.; Rantell, T.; Derbyshire, F. & Chen, Y. et al. (1999). Nanotube composite carbon fibers. *Applied Physics Letters*, vol. 75, No. 9, pp 1329-3, ISSN 0003-6951
- Ashby, M.F. (1996). MOdelling of materials problem. *Journal of Computer-Aided Materials Design*. Vol. 3, No. 1-3, pp.95-99, ISSN 0928-1045
- Balasubramanian, K. & Burghard, M. (2005). Chemically functionalized carbon nanotubes. *Small*, vol. 1, No. 2, pp. 180-192, ISSN 1613-6829
- Banerjee, S.; Hemraj-Benny, T. & Wong, S.S. (2005). Covalent Surface Chemistry of Single-Walled Carbon Nanotubes. *Advanced Materials*, vol. 17, No. 1, pp. 17-29, ISSN 0935-9648
- Banhart, F. (1999). Irradiation effects in carbon nanostructures. *Reports on Progress in Physics*, vol. 62, No. 8, pp. 1181, ISSN 0034-4885
- Batra, R.C. & Sears, A. (2007). Uniform radial expansion/contraction of carbon nanotubes and their transverse elastic moduli. *Modelling and Simulation in Material Science and Engineering*, vol. 15, No. 8, 835, ISSN 0965-0393
- Belytschko, T.; Xiao, S.P.; Schatz, G.C. & Ruoff, R.S. (2002). Atomistic simulations of nanotube fracture. *Physical Review B*, vol. 65, No. 23, pp. 235430-8, ISSN 1050-2947
- Berendsen, H.J.C.; Postma, J.P.M.; van Gunsteren, W.F.; DiNola, A. & Haak, J. R. (1984). Molecular dynamics with coupling to an external bath. *Journal of Chemical Physics*, vol. 81, No. 8, pp. 3684-3690, ISSN 0021-9606
- Bethune, D.S.; Kiang, C. H.; De Vries, M. S.; Gorman, G.; Savoy, R. & Vazquez, J. et al. (1993). Cobalt-catalyzed growth of carbon nanotubes with single-atomic-layer walls. *Nature*, vol. 363, pp. 605-607, ISSN 0028-0836
- Brenner, D. W.; Shenderova, O.A.; Harrison, J.A.; Stuart, S.J.; Ni, B. & Sinnott, S.B. (2002). A second-generation reactive empirical bond order (REBO) potential energy expression for hydrocarbons. *Journal of Physics: Condensed Matter*, vol. 14, No. 4, 783-802, ISSN 1098-0121
- Buehler, M.J. (2008). *Atomistic Modeling of Material Failure*. Springer Science and Business Media, ISBN 978-0-387-76425-2, New York, USA
- Canto, E. D.; Flavin, K.; Movia, D.; Navio, C.; Bittencourt, C. & Giordani, S. (2011). A Critical Investigation of Defect Site Functionalization on Single Walled Carbon Nanotubes. *Chemistry of Materials*, vol. 23, No. 1, pp. 67-74, ISSN 0897-4756
- Chae, H.G.; Minus, M. L. & Kumar, S. (2006). Oriented and Exfoliated Single Wall Carbon Nanotubes in Polyacrylonitrile. *Polymer*, vol. 47, No. 10, pp. 3494-3504, ISSN 0032-3861

- Chandra, N.; Namilae, S. & Shet, C. (2004). Local elastic properties of carbon nanotubes in the presence of Stone-Wales defects. *Physical Review B*, vol. 69, No. 9, pp. 094101-12
- Chou, T. W.; Gao, L.; Thostenson, E.T.; Zhang, Z. & Byun, J.H. (2010). An assessment of the science and technology of carbon nanotube-based fibers and composites. *Composites Science and Technology*, vol. 70, No.1, pp. 1-19, ISSN 0266-3538
- Coluci, V.R.; Pugno, N.M.; Dantas, S.O.; Galvao, D.S. & Jorio, A. (2007). Atomistic simulations of the mechanical properties of 'super' carbon nanotubes. *Nanotechnology*, vol 18, No. 33, pp. 335702, ISSN 1550-7033
- Dalton, A.B.; Collins, S.; Muñoz, E.; Razal, J.M.; Ebron, V.H. & Ferraris, J.P. et al. (2003). Super-tough carbon nanotube fiber. *Nature*, vol. 423, No. 6941, pp. 703-703, ISSN 0028-0836
- Demczyk, B.G.; Wang, Y.M.; Cumings, J.; Hetman, M.; Han, W. & Zettl, A. et al. (2002). Direct mechanical measurement of the tensile strength and elastic Modulus of multiwalled carbon nanotubes. *Materials Science and Engineering A*, vol. 334, pp. 173-178, ISSN 0921-5093
- Dereli, G. & Özdoğan, C. (2003). Structural stability and energetics of single walled carbon nanotubes under uniaxial strain. *Physical Review B*, vol. 67, pp. 035416-11
- Despres, J. F.; Daguerre, E. & Lafdi, K. (1995). Flexibility of graphene layers in carbon nanotubes, *Carbon*, vol. 33, No. 1, pp. 87-92, ISSN 0008-6228
- Ebbesen, T. W. & Ajayan, P. M. (1992). Large scale synthesis of carbon nanotubes. *Nature*, vol. 358, pp. 220-222, ISSN 0028-0836,
- Ebbesen, T. W. & Takada, T. (1995). Topological and SP³ defect structures in nanotubes. *Carbon*, vol. 33, No. 7, pp. 973-978, ISSN 0008-6223
- Eklund, P.C.; Pradhan, B.K.; Kim, U.J.; Xiong, Q.; Fischer, J.E. & Friedman, A.D. et al. (2002). Large scale production of single-walled carbon nanotubes using ultrafast pulses from a free electron laser. *Nano Letters*, vol. 2, No. 6, pp. 561-566, ISSN 1530-6984
- Fan, Y.; Goldsmith, B. R. & Collins, P. G. (2005). Identifying and counting point defects in carbon nanotubes. *Nature Materials*, vol. 4, pp. 906-8911, ISSN 1476-1122
- Felten, A.; Gillon, X.; Gulas, M.; Pireaux, J. J. ; Ke, X. & Tendeloo, G.V. et al. (2010). Measuring Point Defect Density in Individual Carbon Nanotubes Using Polarization-Dependent X-ray Microscopy. *ACS Nano*, vol. 4, No. 8, pp. 4431-6, ISSN 1936-0851
- Guo, T.; Nikolaev, P.; Thess, A.; Colbert, D. T. & Smalley, R. E. (1995). Catalytic growth of single-walled manotubes by laser vaporization. *Chemical Physics Letter*, vol. 243, No.s 1-2, pp. 49-54, ISSN 0009-2614
- Haskins, R.W.; Maier, R.S.; Ebeling, R.M.; Marsh, C.P.; Majure, D.L. & Bednar, A.J. et al. (2007). Tight-binding molecular dynamics study of the role of defects on carbon nanotube moduli and failure. *Journal of Chemical Physics*, vol. 127, No. 7, pp. 074708, ISSN 0021-9606
- Henrard, L.; Loiseau, A.; Journet, C. & Bernier, P. (2000). *European Physical Journal B*. vol. 13, No. 4, pp. 661-669, ISSN 1434-6028
- Hou, W. & Xiao, S. (2007). Mechanical Behaviors of Carbon Nanotubes with Randomly Located Vacancy Defects *Journal of Nanoscience and Nanotechnology*, Vol. 7, No. 12, pp. 4478-4485, ISSN 1550-7033

- Huq, A.M.A.; Goh, K.L.; Zhou, Z.R. & Loao, K. (2008). On defect interactions in axially loaded single-walled carbon nanotubes. *Journal of Applied Physics*, vol. 103, No. 5, pp. 054306-7, ISSN: 0021-8979
- Iijima, S. (1991). Helical microtubules of graphitic carbon. *Nature*, vol. 354, pp. 56-58, ISSN 0028-0836
- Iijima, S.; Brabec, C.; Maiti, A. & Bernholc, J. (1996). Structural flexibility of carbon nanotubes, *Journal of Chemical Physics*, vol. 104, No. 5, pp. 2089-2092, ISSN 0021-9606
- Jorio, A.; Filho, A.G.S.; Dresselhaus, G.; Dresselhaus, M.S.; Saito, R. & Hafner, J. H. et al. (2001). Joint density of electronic states for one isolated single-wall carbon nanotube studied by resonant Raman scattering. *Physical Review B*. vol. 63, No. 24, pp. 245416-4, ISSN 0163-1829
- Kang, H.; Lim, S.; Park, N.; Chun, K.Y. & Baik, S. (2010). Improving the sensitivity of carbon nanotube sensors by benzene functionalization. *Sensors and Actuators B: Chemical*, vol. 147, No. 1, pp. 316-321, ISSN 0925-4005
- Kearns, J.C. & Shambaugh, R.L. (2002). Polypropylene fibers reinforced with carbon nanotubes. *Journal of Applied Polymer Science*, vol. 86, No. 8, pp.2079-2084, ISSN 0021-8995
- Koziol, K.; Vilatela, J.; Moisala, A.; Motta, M.; Cunniff, P.; Sennett, M. & Windle, A. (2007). High-Performance Carbon Nanotube Fiber. *Science*, vol. 318, No. 5858, pp. 1892-1895, ISSN 0965-0393
- Krasheninnikov, A.V. & Banhart, F. (2007). Engineering of nanostructured carbon materials with electron or ion beams, *Nature Materials*, vol. 6, pp. 723-733, ISSN 1476-1122
- Krishnan, A.; Dujardin, E.; Ebbesen, T.W., Yianilos, P.N. & Treacy, M.M.J. (1998). Young's modulus of single-walled nanotubes. *Physical Review B*, vol. 58, No. 20, pp. 14013-14019, ISSN 0163-1829
- Kuronuma, Y.; Shindo, Y.; Takeda, T. & Narita, F. (2010). Fracture behaviour of cracked carbon nanotube-based polymer composites: Experiments and finite element simulations. *Fatigue and Fracture of Engineering Materials and Structures*, vol. 33, No. 2, pp. 87-93, ISSN 8756-758X
- Lennard-Jones, J.E. (1924). On the Determination of Molecular Fields-II, Proceedings of Royal Society of London A, vol. 106, No. 738, pp. 463-477, ISSN 0950-1207
- Liew, K.M.; Wong, C.H.; He, X.Q.; Tan, M.J. & Meguid, S.A. (2004). Nanomechanics of single and multiwalled carbon nanotubes. *Physical Review B*, vol. 69, No. 11, pp. 115429-8, ISSN 0163-1829
- Lourie, O. & Wagner, H D. (1998). Transmission electron microscopy observations of fracture of single-wall carbon nanotubes under axial tension, *Applied Physics Letters*, vol. 73 No. 24, pp. 3527
- Mielke, S. L.; Troya, D.; Zhang, S.; Li, J.L.; Xiao, R.C. & Ruoff, R.S. et al.. (2004). The role of vacancy defects and holes in the fracture of carbon nanotubes. *Chemical Physics Letters*, vol. 390, pp 413-420 ISSN 0009-2614
- Miyamoto, Y.; Rubio, A.; Berber, S.; Yoon, M. & Tomanek, D. (2004). Theoretical identification of Stone-Wales defects in nanotubes. *Physical Review B*, vol. 69, pp. 121413-4, 0163-1829

- Miyata, Y.; Mizuno, K. & Kataura, H. (2011). Purity and Defect Characterization of Single-Wall Carbon Nanotubes Using Raman Spectroscopy. *Journal of Nanomaterials*, doi:10.1155/2011/786763, ISSN 1687-4129
- Mora, R.J.; Vilatela, J.J. & Windle, A. (2009). Properties of composites of carbon nanotube fibres. *Composites Science and Technology*, vol. 69, No 10, pp. 1558-1563, ISSN 0266-3538
- Nardelli, M.B.; Yakobson, B.I. & Bernholc, J. (1998). Mechanism of strain release in carbon nanotubes. *Physical Review B*, vol. 57, No. 8, pp. R4277-R4280, ISSN 0163-1829
- O'Connell, M.J.; Bachilo, S.M.; Huffman, C.B.; Moore, V.C.; Strano, M.S. & Haroz, E.H. et al. (2002). Band Gap Fluorescence from Individual Single-Walled Carbon Nanotubes. *Science*, vol. 297, No. 5581, pp. 593-596, ISSN 0036-8075
- Ouyang, M.; Huang, J.-L.; Cheung, C.L. & Lieber, C.M. (2001). Energy Gaps in "Metallic" Single-Walled Carbon Nanotubes. *Science*, vol. 292 No. 5517, pp. 702-705, ISSN 0036-8075
- Ozaki, T.; Iwasa, Y. & Mitani, T. (2000). Stiffness of single-walled carbon nanotubes under large strain. *Physical Review Letters*, vol. 84, No. 8, pp. 1712-1715, ISSN 0031-9007
- Picozzi, S.; Santucci, S.; Lozzi, L.; Valentini, L. & Delley, D. (2004). Ozone adsorption on carbon nanotubes: the role of Stone-Wales defects. *Journal of Chemical Physics*, vol. 120, No. 5, 7147-7152, ISSN 0021-9606
- Pozrikidis, C. (2009). Effect of the Stone-Wales defect on the structure and mechanical properties of single-wall carbon nanotubes in axial stretch and twist. *Archive of Applied Mechanics*, vol. 79, No. 2, pp.113-123, ISSN 0939-1533
- Qi, P.; Vermesh, O.; Grecu, M.; Javey, M.; Wang, Q. & Dai, H. et al. (2003). Toward Large Arrays of Multiplex Functionalized Carbon Nanotube Sensors for Highly Sensitive and Selective Molecular Detection. *Nano Letters*, vol. 3, No. 3, pp. 347-351, ISSN 1530-6984
- Rahman, A. (1964). Correlations in the Motion of Atoms in Liquid Argon. *Physical Review A*, vol. 136, No. 2A, pp. A405-A411, ISSN 1050-2947
- Reich, S.; Thomsen, C. & Ordejon, P. (2002). Electronic band structure of isolated and bundled carbon nanotubes. *Physical Review B*, vol. 65, No. 15, pp. 155411-11
- Rodríguez-Manzo, J. A.; Tolvanen, A. ; Krasheninnikov, A. V.; Nordlund, K.; Demortière, A. & Banhart, F. (2010). Defect-induced junctions between single- or double-wall carbon nanotubes and metal crystals. *Nanoscale*, vol. 2, No. 6, pp. 901-905. ISSN 2040-3364
- Salvetat, J.-P.; Kulik, A.J.; Bonard, J.-M.; Briggs, G.A.D.; Stöckli, T. & M'et'enier, K. et al. (1999a). Elastic modulus of ordered and disordered multiwalled carbon nanotubes. *Advanced Materials*, vol. 11, No. 2, pp. 161-165, ISSN 0935-9648, ISSN 0935-9648
- Salvetat, J.-P. ; Briggs, G.A.D.; Bonard, J.-M.; Bacsá, R.R.; Kulik, A.J. & Stöckli, T. et al. (1999b). Elastic and shear moduli of single-walled carbon nanotube ropes. *Physical Review Letters*, vol. 82, No. 5, pp. 944-947, ISSN 0031-9007
- Samsonidze, Ge. G.; Samsonidze, G.G. & Yakobson, B.I. (2002). Energetics of Stone-Wales defects in deformations of monoatomic hexagonal layers. *Computational Materials Science*, vol. 23, pp. 62-72, ISSN 0927-0256

- Seo, M.K.; Byun, J.H. & Park, S.J. (2010). Studies on Morphologies and Mechanical Properties of Multi-walled Carbon Nanotubes/Epoxy Matrix Composites. *Bull. Korean Chem. Soc*, vol. 31, No. 5, 1237-1240, ISSN 0253-2964
- Shtogun, Y.V. & Woods, Y.V. (2010). Mechanical properties of defective single wall carbon nanotubes. *Journal of Applied Physics*, vol. 107, No. 6, pp. 061803-6, ISSN 0021-8979
- Song, J.; Jinag, H. & Shi, D.L. (2006). Stone-Wales transformation: Precursor of fracture in carbon nanotubes. *International Journal of Mechanical Science*, vol. 48, No. 12, pp. 1464-1470, ISSN 0965-0393
- Stone, A.J. & Wales, D.J. (1986). Theoretical studies of icosahedral C₆₀ and some related species. *Chemical Physics Letters*, vol. 128, No. 5-6, 501-503, ISSN 0009-2614
- Terrones, M.; Banhart, F.; Grobert, N.; Charlier, J.-C.; Terrones, H. & Ajayan, P. M. (2002). Molecular junctions by joining single-walled carbon nanotubes. *Physical Review Letters*, vol. 89, No. 7, pp. 075505-4, ISSN 0031-9007
- Thess, A.; Lee, R.; Nikolaev, P.; Dai, H.; Petit, P. & Robert, J. et al. (1996). Crystalline ropes of metallic carbon nanotubes. *Science*, vol. 273, No. 5274, pp. 483-487, ISSN 0036-8075
- Treacy, M M J.; Ebbesen, T.W.; Gibson, J.M. (1996). Exceptional high Young's modulus. observed for individual carbon nanotubes, *Nature*, vol. 381, No. 6584, pp. 678-680, ISSN 0028-0836
- Troya, D.; Mielke, S.L. & Schatz, G.C. (2003). Carbon nanotube fracture - differences between quantum mechanical mechanisms and those of empirical potentials. *Chemical Physica Letters*. Vol. 382, No. 1-2, pp. 133-141
- Tunvir, K.; Kim, A. & Nahm, S.H. (2008). The effect of two neighboring defects on the mechanical properties of carbon nanotubes. *Nanotechnology*, vol. 19, No. 6, pp. 065703, ISSN 1550-7033
- Yoon, M.; Han, S.; Kim, G.; Lee, S.B.; Berber, S.; Osawa, I.E. & Ihm, J. et al. (2004). Zipper Mechanism of Nanotube Fusion: Theory and Experiment. *Physical Review Letters*, vol. 92, No. 7, pp. 075504-4, ISSN 0031-9007
- Wang, Q.; Duan, W.H.; Richards, N.L. & Liew, K.M. (2007). Modeling of fracture of carbon nanotubes with vacancy defect. *Physical Review B*, vol. 75, No.-20, pp. 201405(R)-4, ISSN 0163-1829
- Wildoer, J.W.G.; Venema, L.C.; Rinzler, A.G.; Smalley, R.E. & Dekker, C. (1998). Electronic structure of atomically resolved carbon nanotubes. *Nature*, vol. 391, pp. 59-62, ISSN 0028-083
- Wong, E.W.; Sheehan, P.E. & Lieber, C.M. (1997). Nanobeam mechanics : Elasticity, strength and toughness of nanorods and nanotubes. *Science*, vol. 277, No. 5334, pp. 1971-1975, ISSN 0036-8075
- Yakobson, B.I.; Brabec, C.J. & Bernholc, J. (1996). Nanomechanics of Carbon Tubes: Instabilities beyond Linear Response. *Physical Review Letters*, vol. 76, No. 14, 2511-2514, ISSN 0031-9007
- Yang, M. Koutsos, V. & Zaiser, M. (2007). Size effect in the tensile fracture of single-walled carbon nanotubes with defects. *Nanotechnology*, vol. 18, No. 15, 155708, ISSN 1550-7033
- Yip, S. (2005) Lecture notes, MIT, URL-
<http://ocw.mit.edu/courses/nuclear-engineering/22-a09-career-options-for-biomedical-research-fall-2006/lecture-notes/advisorsem05.pdf>, Last accessed on 13-4-2011

- Yu, M.F.; Dyer, M.J.; Skidmore, G.D.; Rohrs, H.W.; Lu, X.K. & Ausman, K.D. et al. (1999a). Three-dimensional manipulation of carbon nanotubes under a scanning electron microscope. *Nanotechnology*, vol. 10, No. 3, pp. 244, ISSN 1550-7033
- Yu, M.F.; Lourie, O.; Dyer, M.J.; Molony, K.; Kelly, T.F. & Ruoff, R.S. (2000b). Strength and Breaking Mechanism of Multiwalled Carbon Nanotubes Under Tensile Load. *Science*, vol. 287, No. 5453, pp. 637-640, ISSN 0036-8075
- Yu, M.F.; Files, B.S.; Arepally, S. & Ruoff, R.S. (2000c). Tensile Loading of Ropes of Single Wall Carbon Nanotubes and their Mechanical Properties. *Physical Review Letters*, vol. 84, No. 24, pp. 5552-5555, ISSN 0031-9007
- Zhang, P.; Lamert, P.E. & Crespi, V.H. (1998). Plastic deformations of carbon nanotubes. *Physical Review Letters*, vol. 81, No. 24, pp. 5346-5349, ISSN 0031-9007

IntechOpen



Carbon Nanotubes - Synthesis, Characterization, Applications

Edited by Dr. Siva Yellampalli

ISBN 978-953-307-497-9

Hard cover, 514 pages

Publisher InTech

Published online 20, July, 2011

Published in print edition July, 2011

Carbon nanotubes are one of the most intriguing new materials with extraordinary properties being discovered in the last decade. The unique structure of carbon nanotubes provides nanotubes with extraordinary mechanical and electrical properties. The outstanding properties that these materials possess have opened new interesting researches areas in nanoscience and nanotechnology. Although nanotubes are very promising in a wide variety of fields, application of individual nanotubes for large scale production has been limited. The main roadblocks, which hinder its use, are limited understanding of its synthesis and electrical properties which lead to difficulty in structure control, existence of impurities, and poor processability. This book makes an attempt to provide indepth study and analysis of various synthesis methods, processing techniques and characterization of carbon nanotubes that will lead to the increased applications of carbon nanotubes.

How to reference

In order to correctly reference this scholarly work, feel free to copy and paste the following:

Keka Talukdar and Apurba Krishna Mitra (2011). Molecular Dynamics Simulation Study on the Mechanical Properties and Fracture Behavior of Single-Wall Carbon Nanotubes, Carbon Nanotubes - Synthesis, Characterization, Applications, Dr. Siva Yellampalli (Ed.), ISBN: 978-953-307-497-9, InTech, Available from: <http://www.intechopen.com/books/carbon-nanotubes-synthesis-characterization-applications/molecular-dynamics-simulation-study-on-the-mechanical-properties-and-fracture-behavior-of-single-wal>

INTECH
open science | open minds

InTech Europe

University Campus STeP Ri
Slavka Krautzeka 83/A
51000 Rijeka, Croatia
Phone: +385 (51) 770 447
Fax: +385 (51) 686 166
www.intechopen.com

InTech China

Unit 405, Office Block, Hotel Equatorial Shanghai
No.65, Yan An Road (West), Shanghai, 200040, China
中国上海市延安西路65号上海国际贵都大饭店办公楼405单元
Phone: +86-21-62489820
Fax: +86-21-62489821

© 2011 The Author(s). Licensee IntechOpen. This chapter is distributed under the terms of the [Creative Commons Attribution-NonCommercial-ShareAlike-3.0 License](#), which permits use, distribution and reproduction for non-commercial purposes, provided the original is properly cited and derivative works building on this content are distributed under the same license.

IntechOpen

IntechOpen